

Heavy-quark contributions to the DIS structure functions F_4 and F_5 at NLO in the ACOT scheme

E. Spezzano,^a T. Ježo,^a M. Klasen,^{a,b} P. Risse,^{c,d} I. Schienbein^e

^a*Institut für Theoretische Physik, Universität Münster, Wilhelm-Klemm-Straße 9, 48149 Münster, Germany*

^b*School of Physics, The University of New South Wales, Sydney NSW 2052, Australia*

^c*Department of Physics, Southern Methodist University, Dallas, TX 75275-0175, U.S.A.*

^d*Jefferson Lab, Newport News, VA 23606, U.S.A.*

^e*Laboratoire de Physique Subatomique et de Cosmologie, Université Grenoble-Alpes, CNRS/IN2P3, 53 Avenue des Martyrs, 38026 Grenoble, France*

E-mail: edoardo.spezzano@uni-muenster.de, tomas.jezo@uni-muenster.de,
michael.klasen@uni-muenster.de, prisse@smu.edu, schien@lpsc.in2p3.fr

ABSTRACT: We compute the contributions of heavy quarks to the deep-inelastic scattering structure functions F_4 and F_5 at next-to-leading order of perturbative QCD in the ACOT scheme. Both analytic results including the details of the calculation as well as numerical results for the neutral and charged current cases are presented. Our study thus lays the groundwork for future measurements of these two structure functions in experiments such as the SHiP experiment.

KEYWORDS: Deep-inelastic scattering, structure functions, perturbative QCD, next-to-leading order, heavy quarks, ACOT scheme, SHiP experiment, APFEL++ implementation

Contents

1	Introduction	1
2	DIS with massive leptons	3
3	Quark scattering	6
3.1	Real contribution	7
3.2	Virtual contribution	9
3.3	Combined contributions	10
3.4	Wilson coefficients and NLO contribution	11
4	Boson-gluon fusion	12
5	Structure functions in the ACOT scheme	14
6	Numerical implementation and results	16
6.1	Neutral-current results	18
6.2	Charged-current results	19
7	Conclusions	21
A	Collinear frame	21
B	$\hat{\mathcal{F}}_2^{\text{QS, NLO}}$	23
C	Plus-distribution identities	23
D	Numerical implementation of the plus distribution	25

1 Introduction

Deep-inelastic scattering (DIS) plays a pivotal role in the understanding of the structure of nucleons and nuclei, as it allows to probe these complex objects composed of quarks and gluons with a point-like test particle (a charged lepton or neutrino) at high energy and resolution. Historically, both theoretical and experimental efforts have predominantly focused on the structure functions F_1 , F_2 , and F_3 [1], while the contributions of the structure functions F_4 and F_5 have been largely ignored. The primary reason for neglecting the structure functions F_4 and F_5 lies in the fact that their contributions to the cross section are suppressed by kinematic prefactors proportional to the square of the incoming and outgoing lepton masses. As a result, they are practically relevant only in processes involving heavy leptons, such as the tau.

Recent advances in experimental techniques may open up new avenues for exploring these previously neglected aspects of the nucleon and nuclear structure. In particular, a five-year run of the Search for Hidden Particles (SHiP) experiment at CERN [2] could provide direct measurements of the structure functions F_4 and F_5 thanks to its unprecedented sensitivity to interactions of the tau lepton and tau neutrino. Furthermore, seven astrophysical tau neutrino candidate events with visible energies from 20 TeV to 1 PeV have recently been observed with the IceCube Neutrino

Observatory [3], and IceCube/DeepCore are investigating their sensitivity to F_4 and F_5 , which increases at lower neutrino energy due to the kinematic prefactors [4]. These experiments therefore have the potential to significantly enhance our understanding of these structure functions and to provide valuable insights into the non-perturbative dynamics in nucleons and nuclei.

In this paper, we present a comprehensive theoretical analysis of the structure functions F_4 and F_5 in anticipation of the forthcoming experimental results. Heavy quarks play a crucial role in DIS, since they contribute significantly to the neutral- and charged-current structure functions at low Bjorken- x . Their production then also offers valuable insights into the gluon and strange quark distributions in the nucleon, which remain poorly constrained by global fits to inclusive DIS data. Theoretical calculations of heavy-quark contributions present a challenge in perturbative QCD, as they require a consistent treatment of mass effects and the resummation of quasi-collinear logarithms. To address this issue, we adopt the Aivazis-Collins-Olness-Tung (ACOT) scheme [5, 6], which provides a systematic framework for incorporating heavy-quark mass effects within a variable flavor number scheme (VFNS) [7]. Specifically, we compute the heavy-quark contributions to F_4 and F_5 up to next-to-leading order (NLO) in the strong coupling, thus providing more precise theoretical predictions to be compared with the upcoming experimental data. It should be noted that the NLO calculation for F_4 and F_5 has already been performed in the fixed flavor number scheme (FFNS) [8]. At this level of precision, only two processes are theoretically allowed for describing the heavy-quark contribution: quark scattering (QS) and boson-gluon fusion (GF). Together, these processes comprehensively capture the contribution of the heavy quark to the structure functions. Both processes have previously been computed for the structure functions F_1 , F_2 , and F_3 in the ACOT scheme at NLO [9]. Here, we extend the work in Ref. [9] to the structure functions F_4 and F_5 . For simplicity, the helicity basis formalism, with which the ACOT scheme was originally formulated, will not be used in this paper. Instead, we will adopt the standard basis, characterized by structure functions F_1, \dots, F_5 , and thus follow the same approach as Ref. [9]. The calculations for both processes were carried out considering a generic $(V - A)$ boson interaction to account for both charged and neutral currents using **FeynCalc** [10–13], a **Mathematica** package for algebraic calculations in quantum field theory.

The remainder of this manuscript is organized as follows:

- [Section 2](#) introduces the kinematic variables relevant for deep-inelastic scattering and presents the hadronic tensor convention adopted in this work together with its decomposition into structure functions.
- [Section 3](#) focuses on the quark scattering process. We present the calculation of the Born, virtual, and real contributions in D space-time dimensions, followed by the derivation of the semi-inclusive and inclusive results.
- [Section 4](#) focuses on the boson-gluon fusion process. This section covers the definition of the process, its Feynman diagrams, kinematics, and the derivation of both semi-inclusive and inclusive results.
- [Section 5](#) presents our final analytical results for the inclusive structure functions in the ACOT scheme.
- [Section 6](#) presents our numerical results. We compare the individual contributions from the GF and QS channels, illustrate their impact on the (x, Q^2) plane, and discuss the significance of heavy-quark contributions and NLO corrections, in particular in the context of SHiP kinematics.

- [Section 7](#) concludes with a summary of our main findings and a discussion of potential directions for future work.

Some technical details of the calculation and the numerical implementation have been relegated to the appendices [A – D](#).

2 DIS with massive leptons

In order to describe the deep-inelastic scattering processes considered in this work, we adopt the standard kinematic variables and conventions for the hadronic tensor as in Ref. [\[1\]](#). The process under study is the scattering of a lepton $\ell_1(k)$ off a nucleon $N(P)$, producing a lepton $\ell_2(k')$ and an inclusive hadronic final state X :

$$\ell_1(k) + N(P) \rightarrow \ell_2(k') + X. \quad (2.1)$$

The four-momentum transfer is defined as $q = k - k'$, and the standard DIS invariants

$$Q^2 = -q^2, \quad x = \frac{Q^2}{2P \cdot q}, \quad y = \frac{P \cdot q}{P \cdot k} \quad (2.2)$$

are introduced, where Q^2 is the virtuality of the exchanged boson, x is the Bjorken scaling variable, and y measures the inelasticity of the process. The nucleon mass is denoted by M .

Depending on the exchanged gauge boson (γ, Z, W^\pm) , the leptonic tensor is given by

$$\begin{aligned} L_{\mu\nu}^\gamma &= 2 \left(-\frac{1}{2}((\mu_1 - \mu_2)^2 + Q^2)g^{\mu\nu} + k^\mu k'^\nu + k'^\mu k^\nu - i\lambda \epsilon^{\mu\nu\alpha\beta} k_\alpha k'_\beta \right), \\ L_{\mu\nu}^{\gamma Z} &= (g_V^e + e\lambda g_A^e) L_{\mu\nu}^\gamma, \\ L_{\mu\nu}^Z &= (g_V^e + e\lambda g_A^e)^2 L_{\mu\nu}^\gamma - 4g_A^e \mu_1 \mu_2 (g_A^e + e\lambda g_V^e) g_{\mu\nu}, \\ L_{\mu\nu}^W &= (1 + e\lambda)^2 L_{\mu\nu}^\gamma - 4(1 + e\lambda) \mu_1 \mu_2 g_{\mu\nu}, \end{aligned}$$

where $g_V^e = -\frac{1}{2} + 2\sin^2\theta_W$, $g_A^e = -\frac{1}{2}$, and μ_1, μ_2 are the masses of the incoming and outgoing leptons, respectively. The parameter λ denotes the helicity of the incoming lepton. For incoming charged leptons in unpolarized DIS, the helicities are averaged over; consequently, the antisymmetric term proportional to $\epsilon^{\mu\nu\alpha\beta}$ cancels. For an incoming neutrino, which is left-handed in the Standard Model, we set $\lambda = -1$; for an incoming antineutrino, which is right-handed, we set $\lambda = +1$.

The hadronic tensor, which encodes the non-perturbative information about the nucleon structure, is conventionally decomposed as

$$W_j^{\mu\nu}(P, q) = -g^{\mu\nu} F_1^j + \frac{P^\mu P^\nu}{P \cdot q} F_2^j - \frac{i\epsilon^{\mu\nu\alpha\beta} P_\alpha q_\beta}{2P \cdot q} F_3^j + \frac{q^\mu q^\nu}{Q^2} F_4^j + \frac{P^\mu q^\nu + q^\mu P^\nu}{2P \cdot q} F_5^j + \frac{P^\mu q^\nu - q^\mu P^\nu}{2P \cdot q} F_6^j, \quad (2.3)$$

where $j = \gamma, \gamma Z, Z, W$ denotes the specific electroweak current contribution (electromagnetic, interference, weak neutral, or charged), and $F_i^j(x, Q^2)$ are the structure functions depending on the Lorentz-invariant kinematic variables x and Q^2 . The number of structure functions appearing in the hadronic tensor is often reduced in real-life calculations, as F_6 is only non-zero if QCD violates time-reversal (or charge-parity) symmetry. Whether F_6 is actually zero can thus be considered an alternative formulation of the strong CP problem of QCD. The coefficients for F_4 and F_5 , and F_6 contain factors of q_μ and q_ν . This implies that their contractions with the leptonic tensor $L_{\mu\nu}$ are proportional to the lepton masses and thus often neglected [\[14\]](#).

The total contraction of the hadronic tensor with the leptonic tensor including the effects of the incoming and outgoing lepton masses μ_1 and μ_2 then leads to the following expressions for the

double-differential cross sections:

$$\frac{d^2\sigma^{\text{NC}}}{dx dy} = \frac{2\pi y\alpha^2}{Q^4} \sum_{k=\gamma, \gamma Z, Z} \eta_k L_k^{\mu\nu} W_{\mu\nu}^k, \quad (2.4)$$

$$\frac{d^2\sigma^{\text{CC}}}{dx dy} = \frac{2\pi y\alpha^2}{Q^4} \eta_W L_W^{\mu\nu} W_{\mu\nu}^W. \quad (2.5)$$

Here, α is the fine-structure constant. The overall prefactor η_k takes into account the specific interaction and is given by

$$\begin{aligned} \eta_\gamma &= 1, & \eta_{\gamma Z} &= \left(\frac{G_F M_Z^2}{2\sqrt{2}\pi\alpha} \right) \left(\frac{Q^2}{Q^2 + M_Z^2} \right), \\ \eta_Z &= \eta_{\gamma Z}^2, & \eta_W &= \frac{1}{2} \left(\frac{G_F M_W^2}{4\pi\alpha} \right)^2 \left(\frac{Q^2}{Q^2 + M_W^2} \right)^2. \end{aligned} \quad (2.6)$$

where G_F is the Fermi constant, and M_Z and M_W are the masses of the Z and W bosons.

In the case of unpolarized incoming charged leptons, the kinematic coefficients associated with the structure functions F_4 and F_5 vanish identically within the γ and γZ sectors. Consequently, these structure functions provide no contribution to the unpolarized neutral-current cross section in these channels.¹ The ZZ exchange channel is therefore the only neutral-current contribution in which F_4 and F_5 may appear for unpolarized beams. However, in the kinematic regime $Q^2 \ll M_Z^2$, this term is heavily suppressed by the propagator factor η_Z . Experimentally, the neutral-current cross section is dominated by the pure electromagnetic contribution, with sub-dominant yet non-negligible γZ interference terms dependent solely on $F_{1,2,3}$. As a result, isolating the suppressed ZZ component, and specifically its dependence on $F_{4,5}$, poses a significant challenge in the absence of polarization.

For completeness, assuming equal lepton masses ($\mu_2 = \mu_1$), the ZZ contribution to the differential cross section is given by:

$$\begin{aligned} \frac{d^2\sigma^{ZZ}}{dx dy} &= \frac{4\pi\alpha^2}{xyQ^2} \eta^{ZZ} \left\{ \frac{xy^2 \left((g_A^e)^2 + (g_V^e)^2 \right) Q^2 + (6(g_A^e)^2 - 2(g_V^e)^2) \mu_1^2}{Q^2} F_1^Z \right. \\ &\quad - \frac{\left((g_A^e)^2 + (g_V^e)^2 \right) ((y-1)Q^2 + M^2 x^2 y^2) Q^2 + 4(g_A^e)^2 M^2 x^2 y^2 \mu_1^2}{Q^4} F_2^Z \\ &\quad \left. - g_A^e g_V^e x y (y-2) F_3^Z + \frac{2(g_A^e)^2 x y^2 \mu_1^2}{Q^2} (F_4^Z - F_5^Z) \right\}. \end{aligned} \quad (2.7)$$

Notably, F_4^Z and F_5^Z enter this expression exclusively through the linear combination $(F_4^Z - F_5^Z)$. This implies that even if the ZZ channel were successfully isolated, the individual structure functions could not be disentangled without additional polarization observables. Given the magnitude of the ZZ suppression in realistic kinematic configurations, the extraction of $F_{4,5}$ from unpolarized neutral-current data is practically infeasible. By contrast, the use of polarized lepton beams provides access to the less-suppressed γZ interference channel, offering a more viable pathway to probe these structure functions

¹For polarized incoming leptons, the γZ interference sector becomes accessible, thereby allowing for the measurement of the associated structure functions in principle.

For the charged current (WW) interaction, relevant for (anti)neutrinos and unpolarized charged leptons the cross section reads

$$\begin{aligned} \frac{d^2\sigma^{WW}}{dx dy} = & \frac{4\pi\alpha^2}{xyQ^2}\tilde{\eta}\eta^W \left\{ \frac{xy^2(Q^2 + \mu_1^2 + \mu_2^2)}{Q^2} F_1^W - \frac{2((y-1)Q^4 + M^2x^2y^2(Q^2 + \mu_1^2 + \mu_2^2))}{Q^4} F_2^W \right. \\ & \mp \frac{xy((2-y)Q^2 + y(\mu_1^2 - \mu_2^2))}{Q^2} F_3^W + \frac{xy^2(\mu_1^4 + (Q^2 - 2\mu_2^2)\mu_1^2 + \mu_2^2(Q^2 + \mu_2^2))}{Q^4} F_4^W \\ & \left. - \frac{2xy((y-1)\mu_1^2 + \mu_2^2)}{Q^2} F_5^W \right\}. \end{aligned} \quad (2.8)$$

Here, $\tilde{\eta} = 2$ for (anti)neutrino scattering, and $\tilde{\eta} = 1$ for unpolarized scattering with charged leptons. The \mp sign in front of F_3^W corresponds to neutrino (positive) versus antineutrino (negative) scattering. In the above expressions one can see, that terms proportional to F_4 and F_5 are always accompanied by factors of the lepton masses μ_1 and μ_2 , so that in the (lepton-)massless limit only F_1 , F_2 , and F_3 contribute, recovering the familiar three-structure-function description of DIS.

In order to extract the individual structure functions from the scattering amplitude, it is necessary to introduce appropriate projectors acting on the hadronic tensor. The projectors associated with F_4 and F_5 are defined as

$$\begin{aligned} P_4^{\mu\nu}(P, q) &= \frac{2Q^2}{\Delta^2} \left(P^2 g^{\mu\nu} + \frac{4}{\Delta^2} \left(\left(\frac{\Delta^2}{2} - 3P^2 Q^2 \right) P^\mu P^\nu + 3P^4 q^\mu q^\nu - P^2 (P \cdot q) (P^\mu q^\nu + q^\mu P^\nu) \right) \right), \\ P_5^{\mu\nu}(P, q) &= -\frac{4(P \cdot q)}{\Delta^2} \left(-\frac{12}{\Delta^2} \left(Q^2 (P \cdot q) P^\mu P^\nu - P^2 (P \cdot q) q^\mu q^\nu + \left(\frac{\Delta^2}{6} - Q^2 P^2 \right) (P^\mu q^\nu + q^\mu P^\nu) \right) \right. \\ &\quad \left. + (P \cdot q) g^{\mu\nu} \right), \end{aligned} \quad (2.9)$$

where

$$\Delta \equiv \Delta((P+q)^2, P^2, -Q^2), \quad \Delta(a, b, c) = \sqrt{a^2 + b^2 + c^2 - 2ab - 2ac - 2bc}. \quad (2.10)$$

These projectors satisfy

$$P_i^{\mu\nu}(P, q) W_{\mu\nu}(P, q) = F_i(x, Q^2), \quad i = 4, 5, \quad (2.11)$$

ensuring the isolation of the desired structure functions. At the parton level, for the quark scattering (QS) and boson-gluon fusion (GF) subprocesses, the corresponding projectors are given by

$$\hat{P}_{i, \text{QS}}^{\mu\nu} \equiv P_i^{\mu\nu}(k_1, q), \quad \hat{P}_{i, \text{GF}}^{\mu\nu} \equiv P_i^{\mu\nu}(p, q), \quad (2.12)$$

where k_1 and p denote the momenta of the incoming quark and gluon, respectively.

It is worth emphasizing that, as shown in eq. (2.9), our calculation of the Wilson coefficients employs the standard four-dimensional projectors for the structure functions. In the conventional massless formalism (see, e.g., Ref. [15]), projectors are formulated in D dimensions to regulate collinear divergences. In our framework, the heavy-quark mass acts as a physical cutoff for such divergences, which validates the use of four-dimensional projectors. At the same time, we maintain a fully D -dimensional treatment of the phase space (*cf.* eq. (3.22)) to regulate soft singularities and to guarantee the correct cancellation of infrared (IR) poles between real and virtual contributions, following the methodology of Ref. [9].

3 Quark scattering

To compute the contribution of the quark scattering process

$$B^*(q) + Q_1(k_1) \rightarrow Q_2(k_2)[+g(p)] \quad (3.1)$$

to the structure functions, we must account for two key components: real emission of an additional gluon and virtual corrections. Here B^* represents a virtual boson (γ, Z, W^\pm) with momentum q , k_1 and k_2 represent the quark momenta for quark with masses m_1 and m_2 , and g is the emitted gluon with momentum p .

For a real emission, the relevant Feynman diagrams are shown in fig. 1. These diagrams represent the processes involving the presence of an additional gluon in the final state and thus contribute to the scattering process at the next-to-leading order. On the other hand, the virtual contribution is represented by the vertex correction, as illustrated in fig. 2. In the on-shell renormalization scheme, self-energy insertions on external fermions legs are exactly canceled by the corresponding mass and wave-function renormalization counterterms and therefore do not appear explicitly in the diagram [16]. These two contributions must be summed at the cross section level to obtain a consistent result [17, 18].

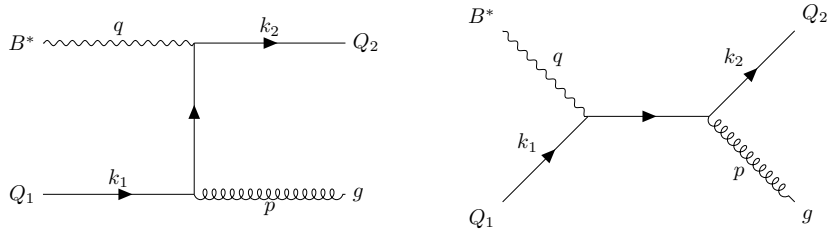


Figure 1: Feynman diagrams relevant for the real contribution at next-to-leading order to the quark scattering process. The emitted gluon is denoted by g .

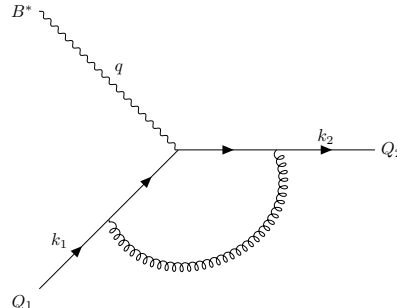


Figure 2: Feynman diagram (triangle vertex correction) relevant for the virtual contribution at next-to-leading order to the quark scattering process.

Since each process involves an external boson, we can write the amplitude in the factorized form

$$\mathcal{M} = \varepsilon_\mu(q) \mathcal{M}^\mu, \quad (3.2)$$

where $\varepsilon_\mu(q)$ denotes the polarization vector of the external gauge boson. Up to phase space integration, the associated partonic tensor is therefore given by

$$\hat{W}_{\mu\nu}^{\text{QS}} = \mathcal{M}_\mu(V, A) (\mathcal{M}_\nu(V', A'))^*, \quad (3.3)$$

where V and A denote the usual vector and axial-vector couplings associated with one current, while V' and A' refer to the corresponding couplings of the second current. So, this general expression is applicable to a variety of interactions, such as those involving interference between different gauge bosons (e.g., γ/Z exchange)².

In order to obtain the hadron level structure functions, we use the set of projectors defined in eq. (2.12).

3.1 Real contribution

By applying the projectors specified in eq. (2.12), the partonic structure functions in the convention of Ref. [9] are defined by

$$\hat{F}_i^{\text{QS}} \equiv \left(C_F \frac{g_s^2}{2} \right)^{-1} \hat{P}_{i, \text{QS}}^{\mu\nu} \overline{\hat{W}_{\mu\nu}^{\text{QS}}}, \quad i = 4, 5, \quad (3.4)$$

where

$$\overline{\hat{W}_{\mu\nu}^{\text{QS}}} = \left(\frac{1}{3} \sum_{\text{color}} \right) \left(\frac{1}{2} \sum_{\text{spins}} \right) \hat{W}_{\mu\nu}^{\text{QS}}. \quad (3.5)$$

In this expression, the factor of $1/3$ originates from averaging over the color states of the incoming quark, while the factor of $1/2$ reflects averaging over its spin states. Semi-inclusively, *i.e.*, without integrating over the phase space of the final state quark, we have

$$\begin{aligned} \hat{F}_4^{\text{QS}}(\hat{s}_1, \hat{t}_1) = & -16 \frac{Q^2}{\Delta'^4} \left\{ q_+ \left[2\Delta^2 m_1^2 + \Sigma_{++}^2 (7m_1^2 + 2m_2^2 - Q^2) + \hat{s}_1 (-2\Delta^2 + 14m_1^2 \Sigma_{++} - \Sigma_{+-}^2) + \frac{4\Delta^2 m_2^2 m_1^2}{\hat{s}_1} \right. \right. \\ & + \hat{s}_1^2 (2m_1^2 - 3\Sigma_{+-}) + \frac{m_1^2 \hat{s}_1 (11\Delta^2 + 36m_1^2 m_2^2 - \Sigma_{+-} \Sigma_{++})}{\hat{t}_1} + \frac{4\Delta^2 m_1^4 \hat{s}_1}{\hat{t}_1^2} + \frac{4m_1^4 \hat{s}_1^2 (2\Sigma_{++} - m_1^2)}{\hat{t}_1^2} \\ & + \frac{6m_2^2 m_1^2 \Sigma_{++} \hat{t}_1}{\hat{s}_1} + \frac{4m_1^2 \hat{s}_1^2 (m_1^2 + 2\Sigma_{++})}{\hat{t}_1} + \frac{4m_1^4 \hat{s}_1^3}{\hat{t}_1^2} + \frac{2m_1^2 \hat{s}_1^3}{\hat{t}_1} - 3m_2^2 \Sigma_{+-}^2 + \frac{4\Delta^2 m_1^2 \Sigma_{++}}{\hat{t}_1} \\ & \left. \left. + \hat{t}_1 (\Sigma_{++} (4m_1^2 - \Sigma_{+-}) + 4m_1^2 m_2^2) - 2\hat{s}_1 \hat{t}_1 \Sigma_{+-} - \hat{s}_1^2 \hat{t}_1 - \hat{s}_1^3 \right] - 2m_1 m_2 q_- \left[\frac{\hat{t}_1 (\Delta^2 + 6m_1^2 m_2^2)}{\hat{s}_1} \right. \right. \\ & \left. \left. + 6m_1^2 \left(\frac{m_1^2 \hat{s}_1}{\hat{t}_1} + \hat{s}_1 + \Sigma_{++} \right) + \hat{t}_1 (2 (m_1^2 + \Sigma_{++}) + \hat{s}_1) \right] \right\} \end{aligned} \quad (3.6)$$

and

²We present the amplitude in this general form for completeness, though it is not strictly required for the results of this work.

$$\begin{aligned}
\hat{F}_5^{\text{QS}}(\hat{s}_1, \hat{t}_1) = & -8 \frac{Q^2}{\hat{x} \Delta'^4} \left\{ q_+ \left[-2\Delta'^2 (5m_1^2 + m_2^2 + 2Q^2) + \hat{t}_1 (\hat{s}_1 (-7m_1^2 - m_2^2 - 3Q^2) - 12m_1^2 m_2^2 + \hat{s}_1^2 \right. \right. \\
& + \Sigma_{++} (\Sigma_{-+} - 4\Sigma_{+-}) + \frac{2\Delta^4 m_2^2}{\hat{s}_1^2} + \hat{s}_1 (-3\Delta^2 - 28m_1^2 m_2^2 - \Sigma_{-+} \Sigma_{++} - 6\Sigma_{+-}^2 + 12\Sigma_{+-} \Sigma_{++}) \\
& - \Sigma_{+-} \Sigma_{++} (7\Sigma_{++} - 4m_2^2) + \Delta^2 (13\Sigma_{++} - 2Q^2) + \frac{2\Delta^4 \Sigma_{++}}{\hat{t}_1 \hat{s}_1} + \frac{2m_1^2 \hat{s}_1^3 (\Sigma_{+-} - 2m_1^2)}{\hat{t}_1^2} \\
& + \frac{4\Delta^2 (2\Delta^2 - m_1^2 \Sigma_{++} + 6m_1^2 m_2^2) + \hat{s}_1^2 (-2\Delta^2 - 20m_1^2 m_2^2 + 4\Sigma_{+-}^2 + 9\Sigma_{+-} \Sigma_{++})}{\hat{t}_1} \\
& + \frac{\hat{s}_1 (\Sigma_{++} (9\Delta^2 - 2m_1^2 \Sigma_{+-} + 4\Sigma_{+-}^2) - 6\Delta^2 m_1^2) + \hat{s}_1^3 (5\Sigma_{+-} - 4m_1^2) + \hat{s}_1^4}{\hat{t}_1} \\
& + \frac{\Delta^2 (5\Delta^2 + 8m_1^2 m_2^2 - 3\Sigma_{-+} \Sigma_{++}) + \hat{t}_1 (\Delta^2 \Sigma_{++} + 2m_2^2 (\Delta^2 - 3\Sigma_{+-} \Sigma_{++}))}{\hat{s}_1} \\
& + \frac{2\Delta^4 m_1^2 + 2m_1^2 \hat{s}_1^2 (\Delta^2 + 2\Sigma_{++} (\Sigma_{+-} - m_1^2) + 4m_1^4) + 2\Delta^2 m_1^2 \hat{s}_1 (3\Sigma_{++} - 2m_1^2)}{\hat{t}_1^2} \Big] \\
& + 2m_1 m_2 q_- \left[2 (3\Sigma_{+-} \Sigma_{++} - \Delta^2) + \frac{6m_1^2 \hat{s}_1 (\hat{s}_1 + \Sigma_{+-})}{\hat{t}_1} + 4\hat{s}_1 (-m_1^2 + \hat{s}_1 + 2\Sigma_{++} + \hat{t}_1) \right. \\
& \left. + 2\hat{t}_1 (3m_2^2 + \Sigma_{+-}) + \frac{\hat{t}_1 (\Delta^2 - 3\Sigma_{-+} \Sigma_{++})}{\hat{s}_1} \right] \Big\}, \tag{3.7}
\end{aligned}$$

where we have defined the quantities

$$q_{\pm} = VV' \pm AA', \quad \Sigma_{\pm\pm} = Q^2 \pm m_2^2 \pm m_1^2, \quad \hat{t}_1 = (k_2 - q)^2 - m_1^2, \quad \hat{s}_1 = (k_1 + q)^2 - m_2^2 \tag{3.8}$$

and

$$\Delta \equiv \Delta(m_1^2, m_2^2, -Q^2), \quad \Delta' \equiv \Delta(m_1^2, \hat{s}_1 + m_2^2, -Q^2), \tag{3.9}$$

with the Δ -function defined in eq. (2.10). Finally, the variable \hat{x} appearing in \hat{F}_5^{QS} can be expressed in terms of \hat{s}_1 using the relation

$$\hat{s}_1 = m_1^2 - m_2^2 + Q^2 \left(\frac{1}{\hat{x}} - 1 \right). \tag{3.10}$$

As a check, we have also recalculated the corresponding expressions for the structure functions $\hat{F}_{1,2,3}^{\text{QS}}(\hat{s}_1, \hat{t}_1)$ and find full agreement with the results in appendix A of Ref. [19].

To obtain the inclusive structure functions, we integrate the semi-inclusive ones over the polar angle θ_{CM} between \vec{k}_2 and \vec{k}_1 in the center-of-mass frame with

$$\hat{F}_i^{\text{QS}}(\hat{s}_1) \equiv \int_0^1 \hat{F}_i^{\text{QS}}(\hat{s}_1, \hat{t}_1(y)) dy, \tag{3.11}$$

where the integration variable y is defined as

$$y = \frac{1}{2} (1 + \cos \theta_{\text{CM}}) \tag{3.12}$$

and $\hat{t}_1(y)$ is given by

$$\hat{t}_1(y) = \frac{\hat{s}_1}{\hat{s}_1 + m_2^2} \Delta'(y - y_0) \tag{3.13}$$

with $y_0 = [1 + (\Sigma_{++} + \hat{s}_1)/\Delta']/2$. Explicitly, the inclusive results can be derived from the semi-inclusive expressions by the following substitutions in eqs. (3.6) and (3.7):

$$\frac{1}{\hat{t}_1^2} \rightarrow \frac{\hat{s}_1 + m_2^2}{m_1^2 \hat{s}_1^2}, \quad \frac{1}{\hat{t}_1} \rightarrow \frac{\hat{s}_1 + m_2^2}{\hat{s}_1 \Delta'} \mathcal{L}, \quad \hat{t}_1 \rightarrow -\frac{\hat{s}_1 (\Sigma_{++} + \hat{s}_1)}{2(\hat{s}_1 + m_2^2)}. \quad (3.14)$$

Here, \mathcal{L} is defined as

$$\mathcal{L} \equiv \ln \left(\frac{\Sigma_{++} + \hat{s}_1 - \Delta'}{\Sigma_{++} + \hat{s}_1 + \Delta'} \right). \quad (3.15)$$

3.2 Virtual contribution

Calculating the vertex correction in fig. 2 in $D = 4 - 2\epsilon$ dimensions and using the Passarino-Veltman decomposition [20], we obtain

$$\begin{aligned} \Gamma_0^\mu = & C_F \frac{\alpha_s}{4\pi} \frac{1}{\Gamma(1-\epsilon)} \left(\frac{Q^2}{4\pi\mu^2} \right)^{-\epsilon} (C_{0,-} \gamma^\mu L_5 + C_+ \gamma^\mu R_5 \\ & + C_{1,-} m_2 k_1^\mu L_5 + C_{1,+} m_1 k_1^\mu R_5 + C_{q,-} m_2 q^\mu L_5 + C_{q,+} m_1 q^\mu R_5) \end{aligned} \quad (3.16)$$

with $L_5 = (V - A\gamma_5)$ and $R_5 = (V + A\gamma_5)$. The coefficients read

$$\begin{aligned} C_{0,-} = & \frac{1}{\epsilon} (1 + \Sigma_{++} I_1) + \left[\frac{\Delta^2}{2Q^2} + \Sigma_{++} \left(1 + \ln \left(\frac{Q^2}{\Delta} \right) \right) \right] I_1 \\ & + \frac{1}{2} \ln \left(\frac{Q^2}{m_1^2} \right) + \frac{1}{2} \ln \left(\frac{Q^2}{m_2^2} \right) + \frac{m_2^2 - m_1^2}{2Q^2} \ln \left(\frac{m_1^2}{m_2^2} \right) + \frac{\Sigma_{++}}{\Delta} \\ & \times \left\{ \frac{1}{2} \ln^2 \left| \frac{\Delta - \Sigma_{+-}}{2Q^2} \right| + \frac{1}{2} \ln^2 \left| \frac{\Delta - \Sigma_{-+}}{2Q^2} \right| - \frac{1}{2} \ln^2 \left| \frac{\Delta + \Sigma_{+-}}{2Q^2} \right| - \frac{1}{2} \ln^2 \left| \frac{\Delta + \Sigma_{-+}}{2Q^2} \right| \right. \\ & \left. - \text{Li}_2 \left(\frac{\Delta - \Sigma_{+-}}{2\Delta} \right) - \text{Li}_2 \left(\frac{\Delta - \Sigma_{-+}}{2\Delta} \right) + \text{Li}_2 \left(\frac{\Delta + \Sigma_{+-}}{2\Delta} \right) + \text{Li}_2 \left(\frac{\Delta + \Sigma_{-+}}{2\Delta} \right) \right\}, \\ C_+ = & 2m_1 m_2 I_1, \\ C_{1,-} = & -\frac{1}{Q^2} \left[\Sigma_{+-} I_1 + \ln \left(\frac{m_1^2}{m_2^2} \right) \right], \\ C_{1,+} = & -\frac{1}{Q^2} \left[\Sigma_{-+} I_1 - \ln \left(\frac{m_1^2}{m_2^2} \right) \right], \\ C_{q,-} = & \frac{1}{Q^4} \left[(\Delta^2 - 2m_1^2 Q^2) I_1 - 2Q^2 + \Sigma_{+-} \ln \left(\frac{m_1^2}{m_2^2} \right) \right], \\ C_{q,+} = & \frac{1}{Q^4} \left[(-\Delta^2 + 2m_2^2 Q^2 - \Sigma_{-+} Q^2) I_1 + 2Q^2 + (\Sigma_{-+} + Q^2) \ln \left(\frac{m_1^2}{m_2^2} \right) \right] \end{aligned} \quad (3.17)$$

with

$$I_1 = \frac{1}{\Delta} \ln \left(\frac{\Sigma_{++} + \Delta}{\Sigma_{++} - \Delta} \right). \quad (3.18)$$

The renormalized vertex is given by

$$\Gamma_R^\mu = \gamma^\mu L_5 (Z_1 - 1) + \Gamma_0^\mu, \quad (3.19)$$

where

$$Z_1 = 1 + C_F \frac{\alpha_s}{4\pi} \frac{1}{\Gamma(1-\epsilon)} \left(\frac{Q^2}{4\pi\mu^2} \right)^{-\epsilon} \left[-\frac{3}{\epsilon} - \frac{3}{2} \ln \left(\frac{Q^2}{m_1^2} \right) - \frac{3}{2} \ln \left(\frac{Q^2}{m_2^2} \right) - 4 \right]. \quad (3.20)$$

The only coefficient that changes after renormalization is $C_{0,-}$, which is replaced by

$$\begin{aligned}
C_{R,-} = & -\frac{1}{\epsilon} (2 - \Sigma_{++} I_1) + \left[\frac{\Delta^2}{2Q^2} + \Sigma_{++} \left(1 + \ln \left(\frac{Q^2}{\Delta} \right) \right) \right] I_1 \\
& + \frac{m_2^2 - m_1^2}{2Q^2} \ln \left(\frac{m_1^2}{m_2^2} \right) - \ln \left(\frac{Q^2}{m_2^2} \right) - \ln \left(\frac{Q^2}{m_1^2} \right) - 4 + \frac{\Sigma_{++}}{\Delta} \\
& \times \left\{ \frac{1}{2} \ln^2 \left| \frac{\Delta - \Sigma_{+-}}{2Q^2} \right| + \frac{1}{2} \ln^2 \left| \frac{\Delta - \Sigma_{-+}}{2Q^2} \right| - \frac{1}{2} \ln^2 \left| \frac{\Delta + \Sigma_{+-}}{2Q^2} \right| - \frac{1}{2} \ln^2 \left| \frac{\Delta + \Sigma_{-+}}{2Q^2} \right| \right. \\
& \left. - \text{Li}_2 \left(\frac{\Delta - \Sigma_{+-}}{2\Delta} \right) - \text{Li}_2 \left(\frac{\Delta - \Sigma_{-+}}{2\Delta} \right) + \text{Li}_2 \left(\frac{\Delta + \Sigma_{+-}}{2\Delta} \right) + \text{Li}_2 \left(\frac{\Delta + \Sigma_{-+}}{2\Delta} \right) \right\}. \tag{3.21}
\end{aligned}$$

These results are in full agreement with Ref. [9].

3.3 Combined contributions

To obtain the final expression for the partonic structure functions, we start by integrating the real semi-inclusive contribution over the phase space, followed by the addition of the virtual contribution. In $D = 4 - 2\epsilon$ dimensions, the phase space is given by [21]

$$d\Pi = \frac{1}{8\pi} \left(\frac{1}{\hat{s}_1^{1+2\epsilon}} \right) \frac{\hat{s}_1^2}{\hat{s}_1 + m_2^2} \frac{1}{\Gamma(1-\epsilon)} \left(\frac{\mu^2}{4\pi(\hat{s}_1 + m_2^2)} \right)^{-\epsilon} y^{-\epsilon} (1-y)^{-\epsilon} dy, \tag{3.22}$$

where we included the renormalization scale μ^2 . The term inside the first parentheses can be reformulated using the identity [22]

$$\frac{1}{\hat{s}_1^{1+2\epsilon}} = -\frac{1}{\Delta^{1+2\epsilon}} \frac{1}{2\epsilon} \delta(1-\xi') + \frac{1}{\hat{s}_1} \frac{1-\xi'}{(1-\xi')_+} + \mathcal{O}(\epsilon), \tag{3.23}$$

where $\xi' \equiv \chi/\xi$ with

$$\chi = \frac{x}{2Q^2} (\Sigma_{+-} + \Delta), \tag{3.24}$$

with x being the Bjorken- x variable defined in eq. (2.2). The identity in eq. (3.23) follows from the expression for \hat{s}_1 , which can be written as

$$\hat{s}_1(\xi') = \frac{1-\xi'}{2\xi'} [(\Delta - \Sigma_{+-})\xi' + \Delta + \Sigma_{+-}], \tag{3.25}$$

derived by combining the expression for \hat{s}_1 given in eq. (3.8) and the scalar products in eq. (A.8). Thus we obtain the expression

$$\hat{\mathcal{F}}_i^{\text{QS, NLO}}(\xi') \equiv \pi \int_0^1 d\Pi \hat{F}_i^{\text{QS}}(\hat{s}_1, \hat{t}_1) + N_i V_i \delta(1-\xi') = N_i (S_i + V_i) \delta(1-\xi') + \frac{1}{8} \frac{1-\xi'}{(1-\xi')_+} \frac{\hat{s}_1}{\hat{s}_1 + m_2^2} \hat{F}_i^{\text{QS}}(\hat{s}_1), \tag{3.26}$$

where $\hat{F}_i(\hat{s}_1)$ are the inclusive structure functions obtained using the substitutions reported in eq. (3.14), and the soft coefficient S_i for $i = 5$ (as well as for $i = 1, 2, 3$ [9]) is defined as

$$S_i = \lim_{\hat{s}_1 \rightarrow 0} \left(\frac{\Delta^2}{m_2^2 Q^2} \right)^{-\epsilon} \left(\frac{1}{\epsilon} \frac{\hat{s}_1^2}{m_2^2} \right) \int_0^1 y^{-\epsilon} (1-y)^{-\epsilon} \left(\frac{m_2^2}{\hat{s}_1^2} + \frac{m_1^2}{\hat{t}_1^2} + \frac{\Sigma_{++}}{\hat{s}_1 \hat{t}_1} \right) dy + \mathcal{O}(\epsilon) \tag{3.27}$$

and $S_4 = 0$. Additionally, we set $\mu^2 = Q^2$ [9] in both eq. (3.16) and eq. (3.22), and following the $\overline{\text{MS}}$ renormalization scheme [23], absorb the Euler–Mascheroni constant along with the 4π factor

into the definition of α_s . Explicitly, the coefficients are given by

$$\begin{aligned}
S_4 &= 0, \\
S_5 &= -\frac{1}{\epsilon}(-2 + \Sigma_{++}I_1) + 2 + \frac{\Sigma_{++}}{\Delta} \left(\Delta I_1 + \text{Li}_2 \left(\frac{2\Delta}{\Delta - \Sigma_{++}} \right) - \text{Li}_2 \left(\frac{2\Delta}{\Delta + \Sigma_{++}} \right) \right) \\
&\quad + \ln \frac{\Delta^2}{m_2^2 Q^2} (-2 + \Sigma_{++}I_1), \\
V_4 &= m_1 \left(m_1 C_{q,+} + \frac{q_-}{q_+} m_2 C_{q,-} \right), \\
V_5 &= C_{R-} + \frac{1}{2} \left((C_{1,+} + C_{q+})m_1^2 + C_{q-}m_2^2 \right) + \frac{q_-}{q_+} \left(\frac{1}{2} m_1 m_2 (C_{1,-} + C_{q,-} + C_{q,+}) + C_+ \right), \\
N_4 &= q_+ \frac{Q^2}{\Delta}, \\
N_5 &= q_+ \frac{\Sigma_{+-}}{\Delta}. \tag{3.28}
\end{aligned}$$

3.4 Wilson coefficients and NLO contribution

To determine the contribution to the structure functions at NLO, it is crucial to first recall the general definition, expressed as a Mellin convolution product [24]

$$F_i^{\text{QS, NLO}} = \frac{\alpha_s}{2\pi} \mathcal{H}_i^{\text{QS, NLO}} \otimes f, \tag{3.29}$$

where f denotes the parton distribution function (PDF) and \mathcal{H}_i are the inclusive Wilson coefficients, also referred to as the coefficient functions. The reason why α_s was introduced instead of g_s^2 lies in the fact that in the definition of the hadronic tensor the normalization factor involving 4π appears [1]:

$$W_{\mu\nu} = \frac{1}{4\pi} \int d^4z e^{iq\cdot z} \langle P | [J_\mu^\dagger(z), J_\nu(0)] | P \rangle. \tag{3.30}$$

Following the same logic adopted for the partonic structure functions, we can define the semi-inclusive Wilson coefficients in the following way [5, 6, 9]:

$$H_i^{\text{QS, NLO}} \equiv \left(\frac{g_s^2}{2} \right)^{-1} P_i^{\mu\nu} \overline{\hat{W}_{\mu\nu}^{\text{QS}}} \Big|_{k_1^+ = \xi P^+}, \quad i = 4, 5 \tag{3.31}$$

with $P^2 = M^2$. In this context, the notation indicates that the scalar products between the hadronic part, arising from the projectors, and the partonic part, originating from the partonic tensor, are determined by imposing proportionality between the plus components of the parton and the nucleon momenta. For a more detailed discussion, we refer to sec. A.

By applying the hadronic projectors, it becomes clear that, in general, there is a mixing between the various partonic structure functions. Specifically, considering the Bjorken limit [25] (i.e. $Q^2 \gg M^2$), we obtain the following relations:

$$\mathcal{H}_4^{\text{QS, NLO}} = C_F \left(\hat{\mathcal{F}}_4^{\text{QS, NLO}} + (\mathcal{R}_2 - 1) \left(\mathcal{R}_1 \hat{\mathcal{F}}_2^{\text{QS, NLO}} + \hat{\mathcal{F}}_5^{\text{QS, NLO}} \right) \right) + \mathcal{O} \left(\frac{M^2}{Q^2} \right), \tag{3.32}$$

$$\mathcal{H}_5^{\text{QS, NLO}} = C_F \mathcal{R}_2 \left(\hat{\mathcal{F}}_5^{\text{QS, NLO}} + 2\mathcal{R}_1 \hat{\mathcal{F}}_2^{\text{QS, NLO}} \right) + \mathcal{O} \left(\frac{M^2}{Q^2} \right), \tag{3.33}$$

where

$$\mathcal{R}_1 = \frac{2m_1^2 \xi'}{\Delta + \Sigma_{+-}}, \quad \mathcal{R}_2 = \frac{m_1^2 + Q^2 \mathcal{R}_1^2}{m_1^2 - Q^2 \mathcal{R}_1^2}. \tag{3.34}$$

Note that we have switched to the phase space integrated version of eq. (3.31). Finally, the leading-order contribution is given by:

$$\begin{aligned}\mathcal{H}_4^{\text{QS, LO}} &= \mathcal{N}_4^{\text{QS, LO}} \delta(1 - \xi'), & F_4^{\text{QS, LO}}(x, Q^2, m_1, m_2) &= \mathcal{N}_4^{\text{QS, LO}} f(\chi) \\ \mathcal{H}_5^{\text{QS, LO}} &= \mathcal{N}_5^{\text{QS, LO}} \delta(1 - \xi'), & F_5^{\text{QS, LO}}(x, Q^2, m_1, m_2) &= \mathcal{N}_5^{\text{QS, LO}} f(\chi)\end{aligned}\quad (3.35)$$

where

$$\begin{aligned}\mathcal{N}_4^{\text{QS, LO}} &= q_+ \frac{4m_1^2 Q^2}{\Delta} \frac{(\Sigma_{++} + \Delta)}{(\Sigma_{+-} + \Delta)^2}, \\ \mathcal{N}_5^{\text{QS, LO}} &= q_+ \frac{m_1^2 - m_2^2 + \Delta}{Q^2},\end{aligned}\quad (3.36)$$

f is the PDF of the incoming quark, and χ is defined in eq. (3.24). The $F_4^{\text{QS, LO}}$ structure function vanishes in the massless limit, consistent with the Albright–Jarlskog relations [26].

Finally, the NLO contribution to the hadron level structure functions is given by:

$$F_i^{\text{QS, NLO}}(x, Q^2, m_1, m_2) = \frac{\alpha_s}{2\pi} \int_{\chi}^1 \frac{d\xi'}{\xi'} \left[f\left(\frac{\chi}{\xi'}, \mu^2\right) \mathcal{H}_i^{\text{QS, NLO}}\left(\xi', \frac{m_1}{Q}, \frac{m_2}{Q}\right) \right]. \quad (3.37)$$

Throughout this work we use the notation $\mathcal{H}(\xi', m_1/Q, m_2/Q)$ for the Wilson coefficients, rather than the more generic form $\mathcal{H}(\xi', Q^2, m_1, m_2)$, as it makes their intrinsic scale invariance manifest. The same convention will be adopted later for the gluon–fusion channel.

4 Boson-gluon fusion

For the boson-gluon fusion process, which appears for the first time at the next-to-leading order,³

$$B^*(q) + g(p) \rightarrow \bar{Q}_1(k_1) + Q_2(k_2), \quad (4.1)$$

the calculations are analogous to the real-emission calculation in the quark scattering case. The semi-inclusive partonic structure functions are defined by [9]

$$\hat{F}_i^{\text{GF}} \equiv \left(\frac{g_s^2}{2\pi}\right)^{-1} \hat{P}_{i, \text{GF}}^{\mu\nu} \overline{\hat{W}_{\mu\nu}^{\text{GF}}}, \quad i = 4, 5, \quad (4.2)$$

where the projectors $\hat{P}_{i, \text{GF}}^{\mu\nu}$ are defined in eq. (2.12) and

$$\overline{\hat{W}_{\mu\nu}^{\text{GF}}} = \left(\frac{1}{8} \sum_{\text{color}}\right) \left(\frac{1}{2} \sum_{\text{pol.}}\right) \sum_{\text{spins}} \hat{W}_{\mu\nu}^{\text{GF}}. \quad (4.3)$$

In this expression, the factor of 1/8 originates from the average over the color states of the incoming gluon, while the factor of 1/2 accounts for averaging over its polarization states.

To determine the contribution of this process, we need to consider the relevant Feynman diagrams, as shown in fig. 3.

³There is no process in the boson-gluon channel at $\mathcal{O}(\alpha_s^0)$, thus it only receives contributions from tree-like Feynman diagrams and there are no diagrams with loops.

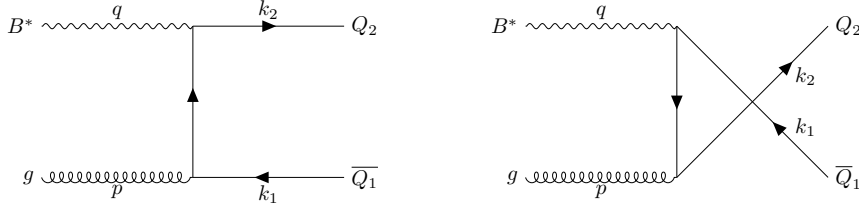


Figure 3: Feynman diagrams relevant for the real contribution at next-to-leading order to the boson-gluon fusion process.

For convenience, the structure functions are expressed in terms of the variables ζ and \hat{x} , where

$$\zeta = \frac{p \cdot k_2}{p \cdot q}, \quad \hat{s} = (q + p)^2 = Q^2 \left(\frac{1}{\hat{x}} - 1 \right). \quad (4.4)$$

Additionally, the amplitude depends on $\hat{u} = (k_2 - p)^2$. The semi-inclusive partonic structure functions can then be decomposed as

$$\hat{F}_i^{\text{GF}}(\zeta, \hat{x}, Q^2) = 8\pi \left(\frac{A_i(\hat{x})}{(1 - \zeta)^2} + \frac{B_i(\hat{x})}{\zeta^2} + \frac{C_i(\hat{x})}{1 - \zeta} + \frac{D_i(\hat{x})}{\zeta} + E_i(\hat{x}) \right) \quad (4.5)$$

where the functions $A_i(\hat{x})$, $B_i(\hat{x})$, $C_i(\hat{x})$, $D_i(\hat{x})$, and $E_i(\hat{x})$ are given by

$$\begin{aligned} A_4 &= 0, \\ B_4 &= 0, \\ C_4 &= -2q_+ \frac{m_1^2}{Q^2} \hat{x}^2, \\ D_4 &= C_4(m_1 \leftrightarrow m_2), \\ E_4 &= -2q_+(\hat{x} - 1)\hat{x}, \\ A_5 &= q_+ \hat{x}^2 \frac{m_1^2}{Q^2} \left(1 + \frac{m_2^2 - 3m_1^2}{Q^2} \right), \\ B_5 &= A_5(m_1 \leftrightarrow m_2), \\ C_5 &= 2q_+ \left(\frac{m_1^4 \hat{x}^2}{2Q^4} - \frac{3m_2^2 m_1^2 \hat{x}^2}{Q^4} + \frac{m_2^4 \hat{x}^2}{2Q^4} + \frac{m_1^2 (3 - 8\hat{x}) \hat{x}}{2Q^2} + \frac{m_2^2 \hat{x} (2\hat{x} - 1)}{2Q^2} + \frac{1}{4} (2(\hat{x} - 1)\hat{x} + 1) \right), \\ D_5 &= C_5(m_1 \leftrightarrow m_2), \\ E_5 &= -q_+ (6\hat{x}^2 - 6\hat{x} + 1). \end{aligned} \quad (4.6)$$

As for the quark scattering process, we integrate over the phase space with

$$\hat{\mathcal{F}}_i^{\text{GF, NLO}}(\hat{x}, Q^2) \equiv \frac{1}{8\pi} \int_{\zeta_-}^{\zeta_+} \hat{F}_i^{\text{GF}}(\zeta, \hat{x}, Q^2) d\zeta, \quad (4.7)$$

where the integration boundaries ζ_{\pm} are defined as

$$\zeta_{\pm} = \frac{1}{2} (\zeta_1 \pm \zeta_2) \quad \text{with} \quad \zeta_1 = 1 + \frac{m_2^2 - m_1^2}{\hat{s}}, \quad \zeta_2 = \frac{1}{\hat{s}} \Delta(\hat{s}, m_2^2, m_1^2). \quad (4.8)$$

Using eq. (4.5), we obtain

$$\hat{\mathcal{F}}_i^{\text{GF, NLO}}(\hat{x}, Q^2) = A_i \frac{\zeta_+ - \zeta_-}{(1 - \zeta_+)(1 - \zeta_-)} + B_i \frac{\zeta_+ - \zeta_-}{\zeta_+ \zeta_-} + C_i \ln \left(\frac{1 - \zeta_-}{1 - \zeta_+} \right) + D_i \ln \left(\frac{\zeta_+}{\zeta_-} \right) + E_i(\zeta_+ - \zeta_-). \quad (4.9)$$

Unlike the quark scattering process, in this case there is no mixing, since the initial parton, the gluon, is massless. Therefore, we have

$$\mathcal{H}_i^{\text{GF, NLO}} = \hat{\mathcal{F}}_i^{\text{GF, NLO}}. \quad (4.10)$$

At the hadron level, the NLO contribution arising from the boson-gluon fusion process is then given by the convolution

$$F_i^{\text{GF, NLO}} = \frac{\alpha_s}{2\pi} \mathcal{H}_i^{\text{GF, NLO}} \otimes g, \quad (4.11)$$

where g is the gluon PDF. Explicitly, it takes the form

$$F_i^{\text{GF, NLO}}(x, Q^2, m_1, m_2) = \frac{\alpha_s}{2\pi} \int_{\chi'}^1 \frac{d\xi'}{\xi'} \left[g\left(\frac{\chi'}{\xi'}, \mu^2\right) \mathcal{H}_i^{\text{GF, NLO}}\left(\xi', \frac{m_1}{Q}, \frac{m_2}{Q}\right) \right], \quad (4.12)$$

where

$$\xi' = \frac{\chi'}{x} \hat{x}, \quad \chi' = x \frac{(m_1 + m_2)^2 + Q^2}{Q^2}. \quad (4.13)$$

5 Structure functions in the ACOT scheme

The treatment of heavy quarks in DIS requires a consistent framework that incorporates both mass effects near threshold and the resummation of large logarithms at asymptotically high scales. The ACOT scheme [5, 6] provides such a framework by combining massive Wilson coefficients with DGLAP-evolved parton distribution functions, while introducing explicit subtraction terms to prevent double counting. This construction ensures that structure functions interpolate smoothly between the fixed-flavor-number scheme, where heavy quarks are produced dynamically, and the variable-flavor-number scheme, where heavy quarks are treated as active partons.

The conceptual basis of the ACOT scheme lies in the treatment of heavy quarks within the factorization framework [7]. In a massless scheme, collinear divergences in the partonic cross sections are regulated dimensionally and absorbed into the PDFs, so that heavy-quark parton distributions are generated dynamically through QCD evolution. When the heavy-quark mass is retained in the Wilson coefficients, it acts as a regulator of the collinear behavior, and heavy quarks are then produced explicitly in the hard scattering through processes such as boson-gluon fusion. The factorization scale μ controls the transition between these two descriptions: for $\mu \simeq m_1$, the mass-dependent treatment dominates, while for $\mu \gg m_1$, the heavy quark can be treated as a parton with its own distribution $f_{Q_1}(x, \mu^2)$.

Near threshold ($\mu \sim m_1$), the dominant contribution to the heavy-quark distribution arises from gluon splitting:

$$f_{Q_1}(x, \mu^2) \simeq \frac{\alpha_s(\mu^2)}{2\pi} \ln\left(\frac{\mu^2}{m_1^2}\right) P_{qg} \otimes g(x, \mu^2) + \mathcal{O}(\alpha_s^2). \quad (5.1)$$

When this PDF is convolved with the LO quark-scattering coefficient function, a term of apparent $\mathcal{O}(\alpha_s)$ in the structure functions actually appears at $\mathcal{O}(\alpha_s^2)$ (since $f_{Q_1} = \mathcal{O}(\alpha_s)$):

$$F_i^H \simeq \frac{\alpha_s(Q^2)}{2\pi} \ln\left(\frac{Q^2}{m_1^2}\right) \left[\mathcal{H}_i^{\text{QS,LO}} \otimes_{\chi} P_{qq} \otimes f_{Q_1} + \mathcal{H}_i^{\text{QS,LO}} \otimes_{\chi} P_{qg} \otimes g \right], \quad i = 4, 5, \quad (5.2)$$

where P_{qq} and P_{qg} are the usual leading order splitting functions [27] defined as

$$P_{qq}(\xi') = C_F \left[\frac{1 + \xi'^2}{1 - \xi'} \right]_+, \quad P_{qg}(\xi') = \frac{1}{2} [(1 - \xi')^2 + \xi'] \quad (5.3)$$

with the standard convolution [28]

$$(P \otimes f)(x) = \int_x^1 \frac{d\xi'}{\xi'} P(\xi') f\left(\frac{x}{\xi'}\right). \quad (5.4)$$

At genuine NLO, the massive quark-scattering and gluon-fusion coefficient functions develop exactly the same large logarithms in the limit $m_{Q_1} \rightarrow 0$:

$$\lim_{m_1 \rightarrow 0} \mathcal{H}_i^{\text{QS,NLO}} \otimes_{\chi} f_{Q_1} = \frac{\alpha_s}{2\pi} \ln\left(\frac{Q^2}{m_1^2}\right) P_{qq} \otimes f_{Q_1} + \text{finite}, \quad (5.5)$$

$$\lim_{m_1 \rightarrow 0} \mathcal{H}_i^{\text{GF,NLO}} \otimes g = \frac{\alpha_s}{2\pi} \ln\left(\frac{Q^2}{m_1^2}\right) P_{qg} \otimes g + \text{finite}. \quad (5.6)$$

A direct addition of these NLO terms to the LO massive calculation would therefore double-count the resummed logarithms already contained in the heavy-quark PDF.

The ACOT scheme resolves this by subtracting those contributions, that are reproduced by the zero-mass (ZM) limit, from the massive NLO coefficient functions. Precisely we have:

$$F_i^{\text{ACOT}} = F_i^{\text{QS,LO}} + F_i^{\text{QS,NLO}} + F_i^{\text{GF,NLO}} - F_i^{\text{QS,SUB}} - F_i^{\text{GF,SUB}}, \quad i = 4, 5. \quad (5.7)$$

In the following, we present the explicit subtraction terms adopting the conventional scale choice $\mu_R = \mu_F = Q$, as originally derived in the ACOT scheme [6, 7, 9]. This choice serves to simplify the analytic structure of the coefficients by eliminating explicit renormalization scale logarithms in the definition. However, we emphasize that this choice is not mandatory. In modern phenomenological applications and global PDF analyses, more general dynamical scales such as $\mu_{R,F}^2 = Q^2 + cm_Q^2$ or scales proportional to the transverse mass are commonly employed to improve perturbative stability near thresholds and in multi-scale kinematic regions. With this in mind, the subtraction terms for the inclusive case are given by [9, 29]

$$F_i^{\text{QS,SUB}}(x, Q^2, m_1, m_2) = \mathcal{N}_i^{\text{QS,LO}} \frac{\alpha_s(Q^2)}{2\pi} \int_{\chi}^1 \frac{d\xi'}{\xi'} f_{Q_1}\left(\frac{\chi}{\xi'}, Q^2\right) \mathcal{H}_i^{\text{QS,SUB}}\left(\xi', \frac{m_1}{Q}\right), \quad (5.8)$$

$$\mathcal{H}_i^{\text{QS,SUB}}\left(\xi', \frac{m_1}{Q}\right) = c_i C_F \left[\frac{1 + \xi'^2}{1 - \xi'} \left(\ln \frac{Q^2}{m_1^2} - 1 - 2 \ln(1 - \xi') \right) \right]_+, \quad (c_4 = 0, c_5 = 1), \quad (5.9)$$

and for the gluon-fusion channel

$$F_i^{\text{GF,SUB}}(x, Q^2, m_1, m_2) = \mathcal{N}_i^{\text{QS,LO}} \frac{\alpha_s(Q^2)}{2\pi} \int_{\chi}^1 \frac{d\xi'}{\xi'} g\left(\frac{\chi}{\xi'}, Q^2\right) \mathcal{H}_i^{\text{GF,SUB}}\left(\xi', \frac{m_1}{Q}, \frac{m_2}{Q}\right), \quad (5.10)$$

$$\mathcal{H}_i^{\text{GF,SUB}}\left(\xi', \frac{m_1}{Q}, \frac{m_2}{Q}\right) = c_i P_{qg}(\xi') \left[\Theta\left(1 - \frac{m_1^2}{Q^2}\right) \ln \frac{Q^2}{m_1^2} + \Theta\left(1 - \frac{m_2^2}{Q^2}\right) \ln \frac{Q^2}{m_2^2} \right]. \quad (5.11)$$

Here, the Heaviside theta-functions enforce the CWZ decoupling prescription [30]: the subtraction is only active when the factorization scale Q exceeds the heavy quark mass. While the first term subtracts the PDF double-counting associated with the incoming parton m_1 , the inclusion of the m_2 term is necessary to explicitly subtract the collinear singularity arising from the second heavy quark line, ensuring the result is IR safe. Below threshold, the heavy quark is not considered an active parton, and no collinear subtraction is required. The ACOT-renormalized Wilson coefficients are then given by:

$$\mathcal{H}_i^{\text{QS,ACOT}}\left(\xi', \frac{m_1}{Q}, \frac{m_2}{Q}\right) = \mathcal{H}_i^{\text{QS,NLO}}\left(\xi', \frac{m_1}{Q}, \frac{m_2}{Q}\right) - \mathcal{H}_i^{\text{QS,SUB}}\left(\xi', \frac{m_1}{Q}\right), \quad (5.12)$$

$$\mathcal{H}_i^{\text{GF,ACOT}}\left(\xi', \frac{m_1}{Q}, \frac{m_2}{Q}\right) = \mathcal{H}_i^{\text{GF,NLO}}\left(\xi', \frac{m_1}{Q}, \frac{m_2}{Q}\right) - \mathcal{H}_i^{\text{GF,SUB}}\left(\xi', \frac{m_1}{Q}, \frac{m_2}{Q}\right). \quad (5.13)$$

By construction, these coefficient functions are free of large logarithms and smoothly approach the standard massless $\overline{\text{MS}}$ NLO coefficient functions in the double limit $m_1, m_2 \rightarrow 0$:

$$\lim_{m_2 \rightarrow 0} \lim_{m_1 \rightarrow 0} \mathcal{H}_i^{\text{QS,ACOT}}\left(\xi', \frac{m_1}{Q}, \frac{m_2}{Q}\right) = C_{F,i}^{(1)}(\xi'), \quad (5.14)$$

$$\lim_{m_2 \rightarrow 0} \lim_{m_1 \rightarrow 0} \mathcal{H}_i^{\text{GF,ACOT}}\left(\xi', \frac{m_1}{Q}, \frac{m_2}{Q}\right) = C_{G,i}^{(1)}(\xi'). \quad (5.15)$$

The coefficient functions $C_{F/G,i}^{(1)}(\xi')$ were computed previously in Ref. [31] (eqs. (31)–(34)) and are reproduced here for completeness:

$$C_{G,4}^{(1)}(\xi') = 2\xi'(1 - \xi'), \quad (5.16)$$

$$C_{G,5}^{(1)}(\xi') = -1 + 8\xi'(1 - \xi') + [(1 - \xi')^2 + \xi'^2] \ln\left(\frac{1 - \xi'}{\xi'}\right), \quad (5.17)$$

$$C_{F,4}^{(1)}(\xi') = C_F \xi', \quad (5.18)$$

$$C_{F,5}^{(1)}(\xi') = C_F \left[\frac{1 + \xi'^2}{1 - \xi'} \left(\ln\left(\frac{1 - \xi'}{\xi'}\right) - \frac{3}{4} \right) + \frac{1}{4}(9 + 5\xi') \right]_+. \quad (5.19)$$

An immediate consequence of the previous equations is that in the ultrarelativistic ($m_f^2/Q^2 \rightarrow 0$) limit, all explicit mass dependence cancels. In this regime the structure functions satisfy the Albright–Jarlskog relations [26],

$$F_L^{\text{ACOT}}(x, Q^2) = 2x F_4^{\text{ACOT}}(x, Q^2), \quad F_2^{\text{ACOT}}(x, Q^2) = x F_5^{\text{ACOT}}(x, Q^2), \quad (5.20)$$

with $F_L^{\text{ACOT}}(x, Q^2) = F_2^{\text{ACOT}}(x, Q^2) - 2x F_1^{\text{ACOT}}(x, Q^2)$. This relation holds for both neutral-current and charged-current scattering.

In summary, the ACOT scheme provides a theoretically consistent and phenomenologically robust description of the heavy-quark structure functions. It retains exact heavy-quark mass dependence at all orders in the hard-scattering coefficient functions, avoids double counting of logarithmic contributions, and automatically resums heavy quarks collinear logs to all orders via DGLAP evolution. The explicit expressions presented above serve as the foundation for the numerical analysis performed in the following section.

6 Numerical implementation and results

In this section, we discuss explicit numerical results that illustrate important features of the structure functions F_4 and F_5 as well as their relevant kinematics limits of the ACOT scheme. We have implemented NC interactions in **Mathematica** and further the CC interactions for both W^- and W^+ exchange in **Mathematica** and in the C++ library **APFEL++** [32–34]. **APFEL++** provides

a highly optimized setup for the calculation of structure functions by the means of constructing pre-computed tables that allow for rapid numerical evaluations across a wide range of kinematics⁴.

The implementation of the massive F_4 and F_5 structure functions in the ACOT scheme has to be performed on a channel-by-channel basis due to the different flavor and mass dependences in the NC and CC interactions. For the following it is useful to introduce the short-hand notation

$$\mathcal{H}_{i,\alpha,\beta}^{\text{QS/GF},k}(\xi') \equiv \mathcal{H}_i^{\text{QS/GF}}\left(\xi', \frac{m_\alpha}{Q}, \frac{m_\beta}{Q}\right), \quad (6.1)$$

where $\alpha, \beta \in \{u, d, s, c, b, t\}$ and $k = ZZ, WW$ in order to clarify the mass dependence for the individual flavor contributions. The antiparticles are denoted by $\bar{\alpha}$ (with $m_\alpha = m_{\bar{\alpha}}$) and the couplings are given by [35]

$$ZZ, \text{ up-type case : } V = V' = \frac{1}{2} - \frac{4}{3} \sin^2 \theta_W, \quad A = A' = \frac{1}{2}, \quad (6.2)$$

$$ZZ, \text{ down-type case : } V = V' = -\frac{1}{2} + \frac{2}{3} \sin^2 \theta_W, \quad A = A' = -\frac{1}{2}, \quad (6.3)$$

$$WW : \quad V = V' = A = A' = 1. \quad (6.4)$$

Following eq. (5.7), the individual massive contributions at LO, NLO and the subtraction terms are combined into the ACOT scheme as

$$F_{i,\alpha,\beta}^{\text{QS,ACOT},k}(x, Q^2) = F_{i,\alpha,\beta}^{\text{QS,LO},k} + F_{i,\alpha,\beta}^{\text{QS,NLO},k} - F_{i,\alpha,\beta}^{\text{QS,SUB},k}, \quad (6.5)$$

$$F_{i,\alpha,\beta}^{\text{GF,ACOT},k}(x, Q^2) = F_{i,\alpha,\beta}^{\text{GF,NLO},k} - F_{i,\alpha,\beta}^{\text{GF,SUB},k}. \quad (6.6)$$

Then the full neutral-current structure functions are

$$\begin{aligned} F_i^{\text{NC,ACOT}}(x, Q^2) &= \sum_{U=u,c,t} \left[F_{i,U,U}^{\text{QS,ACOT},ZZ} + F_{i,\bar{U},\bar{U}}^{\text{QS,ACOT},ZZ} + 2 F_{i,U,\bar{U}}^{\text{GF,ACOT},ZZ} \right] \\ &+ \sum_{D=d,s,b} \left[F_{i,D,D}^{\text{QS,ACOT},ZZ} + F_{i,\bar{D},\bar{D}}^{\text{QS,ACOT},ZZ} + 2 F_{i,D,\bar{D}}^{\text{GF,ACOT},ZZ} \right]. \end{aligned} \quad (6.7)$$

The factor of two in front of the gluon-fusion terms arises from the symmetry $F_{i,\bar{f},\bar{f}}^{\text{GF,ACOT},ZZ} = F_{i,f,f}^{\text{GF,ACOT},ZZ}$ for any flavor f . For the charged-current case the corresponding expressions are

$$\begin{aligned} F_i^{W^-, \text{ACOT}}(x, Q^2) &= \sum_{U=u,c,t} \sum_{D=d,s,b} |V_{UD}|^2 \left[F_{i,\bar{D},\bar{U}}^{\text{QS,ACOT},WW} + F_{i,U,\bar{D}}^{\text{QS,ACOT},WW} \right. \\ &\quad \left. + F_{i,\bar{D},\bar{U}}^{\text{GF,ACOT},WW} + F_{i,U,\bar{D}}^{\text{GF,ACOT},WW} \right], \\ F_i^{W^+, \text{ACOT}}(x, Q^2) &= \sum_{U=u,c,t} \sum_{D=d,s,b} |V_{UD}|^2 \left[F_{i,D,U}^{\text{QS,ACOT},WW} + F_{i,U,\bar{D}}^{\text{QS,ACOT},WW} \right. \\ &\quad \left. + F_{i,D,U}^{\text{GF,ACOT},WW} + F_{i,\bar{U},\bar{D}}^{\text{GF,ACOT},WW} \right]. \end{aligned} \quad (6.8)$$

The Wilson coefficients for F_4 and F_5 , especially when retaining the quark masses, are not straightforward to evaluate numerically. Since the coefficients not only consist of regular functions, but also of delta- and plus-distributions, a special treatment is required. In the case of plus-distributions, the integration is further complicated, since the integration is not performed over the

⁴We did not implement the NC structure functions in **APFEL++** due to the unusual and phenomenologically less relevant case that only Z -boson exchanges contribute which would require a substantial reorganization of the existing framework and is not justified within the scope of the present study.

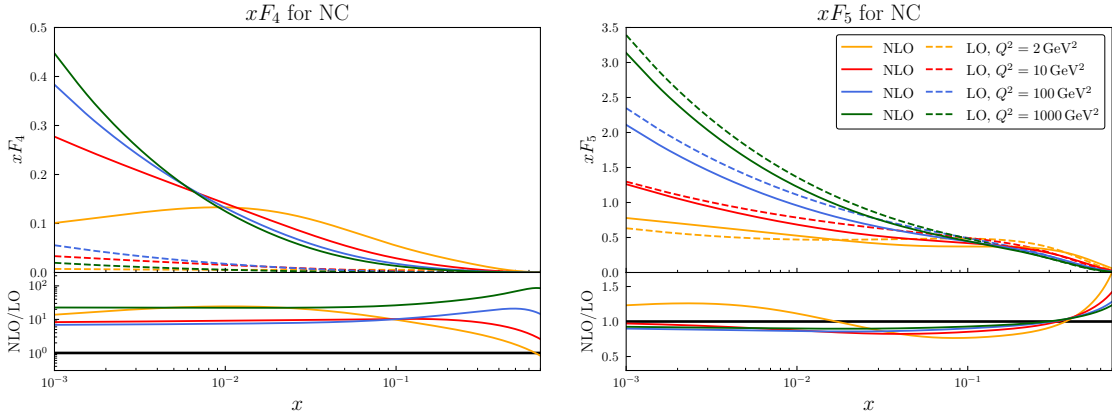


Figure 4: The total structure functions $x F_4$ (left) and $x F_5$ (right) for Z exchange at NLO for various Q^2 values. The LO contributions are given by the dashed lines. The bottom panel shows the NLO over LO ratio on a logarithmic scale for F_4 and on a linear scale for F_5 . Note the difference in the scales between F_4 and F_5 for both the absolute and ratio plots.

interval $[0, 1]$ but $[\chi, 1]$ ⁵. This leads to additional terms in the evaluation of the integrals, see sec. C for a derivation. The numerical treatment along with explicit calculations of the additional terms for F_4 and F_5 can be found in sec. D.

By examining the *unpolarized* NC cross section, *cf.* eq. (2.7), we can see that the contributions from F_4 and F_5 are suppressed by both the lepton mass and the Z propagator such that the cross section is dominated by the structure functions $F_{1,2,3}$ which also receive contributions from the γ and γZ channels. Therefore we discuss the NC results only briefly in the following and focus more on the CC results.

All numerical evaluations use the CT18NLO PDF set [36] accessed via LHAPDF [37] using the masses $m_c = 1.3$ GeV and $m_b = 4.75$ GeV. Contributions from the top quark are neglected in the plots.

6.1 Neutral-current results

We show calculations of the absolute structure functions in fig. 4 with $x F_4$ on the left and $x F_5$ on the right in the range $x \in [10^{-3}, 0.7]$. The upper panels show the NLO (solid) and LO (dashed) curves for $Q^2 \in \{2, 10, 100, 1000\}$ GeV 2 in the colors $\{\text{yellow, red, blue, green}\}$. Note that we choose to plot the structure function multiplied with x , since both are accompanied by x in the cross section. The lower panels depict the NLO/LO ratios. We can see that, both in terms of the absolute scale and the size of the NLO/LO correction, F_4 behaves similar to F_L and F_5 similar to F_2 , as indicated by the AJ relation (*cf.* eq. (5.20)). The shape of F_4 is mainly driven by the gluon contribution at NLO. The LO contribution is suppressed by the quark masses and effectively zero at large Q^2 . On the other hand, F_5 receives only moderate corrections at NLO, and one can see the distinct valence-quark shape at larger x arising from the LO. The NLO corrections can be positive or negative depending on x and Q . The corrections go up to $\pm 25\%$ at lower x and Q . Close to $x = 1$ the relative corrections become very large, where the perturbative series becomes unstable [38, 39] due to $\ln(1 - \chi)$ terms (see sec. D for explicit appearances in F_5). However, the absolute corrections remain small as the structure function strongly tends to zero.

⁵Note that up to NLO plus-distributions only appear in the QS case for $F_{4/5}$, therefore the relevant lower integration limit here is χ .

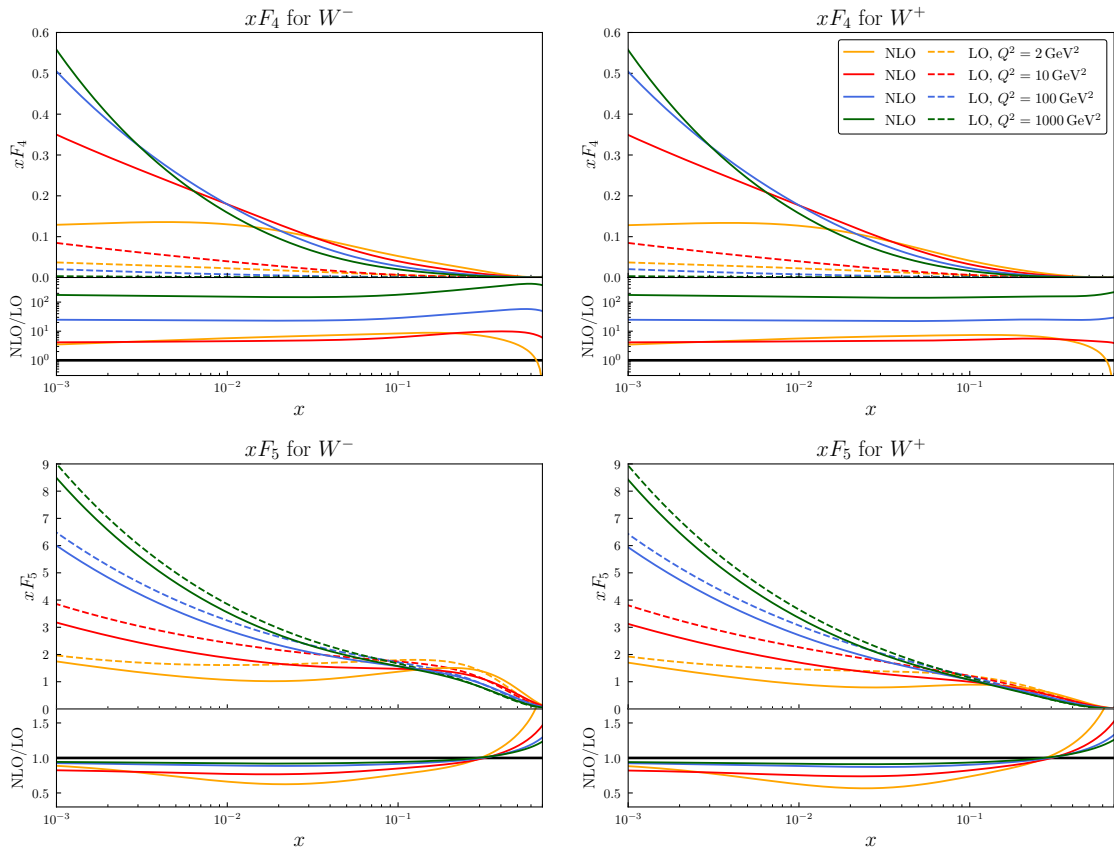


Figure 5: Same as fig. 4 but for CC. We show xF_4 in the top row and xF_5 in the bottom row for W^- exchange in the left column and W^+ exchange in the right column.

6.2 Charged-current results

The CC structure functions given in the same format as for the NC case are shown in fig. 5. The top row shows xF_4 , and the bottom row xF_5 . On the left hand side (here and in the following figures) we assume W^- exchange and W^+ exchange on the right hand side. Comparing this figure to the NC results, we note generally the same behavior: F_4 is dominated by the gluon contribution and receives large NLO corrections, whilst F_5 is mainly given by the quarks from the leading order QS. For the latter in CC the NLO corrections can be larger and yield up to $\sim 45\%$. If we compare the predictions for W^- and W^+ exchanges, we observe differences originating from the flavor structure. The GF contribution is the same for W^- and W^+ and therefore we find the strongest differences for F_5 . We see that the valence bump is more pronounced for W^- , since it probes the up-quark and W^+ the down-quark. Here, we have chosen the proton as the hadron. The difference would be reversed, if we were to choose a neutron as the target, and reduced (or completely removed) for (isoscalar) nuclei. In the sea-quark region, at lower x , we find the same F_5 for both W^- and W^+ as the difference between up- and down-type quarks vanishes.

To illustrate the mass dependence of our results we now turn to ratios to the zero-mass expressions for both structure functions. Due to the AJ relation, with $2xF_4|_{ZM} = F_L|_{ZM}$ and $xF_5|_{ZM} = F_2|_{ZM}$, these ratios also show the convergence towards the more familiar $F_{L/2}$ structure

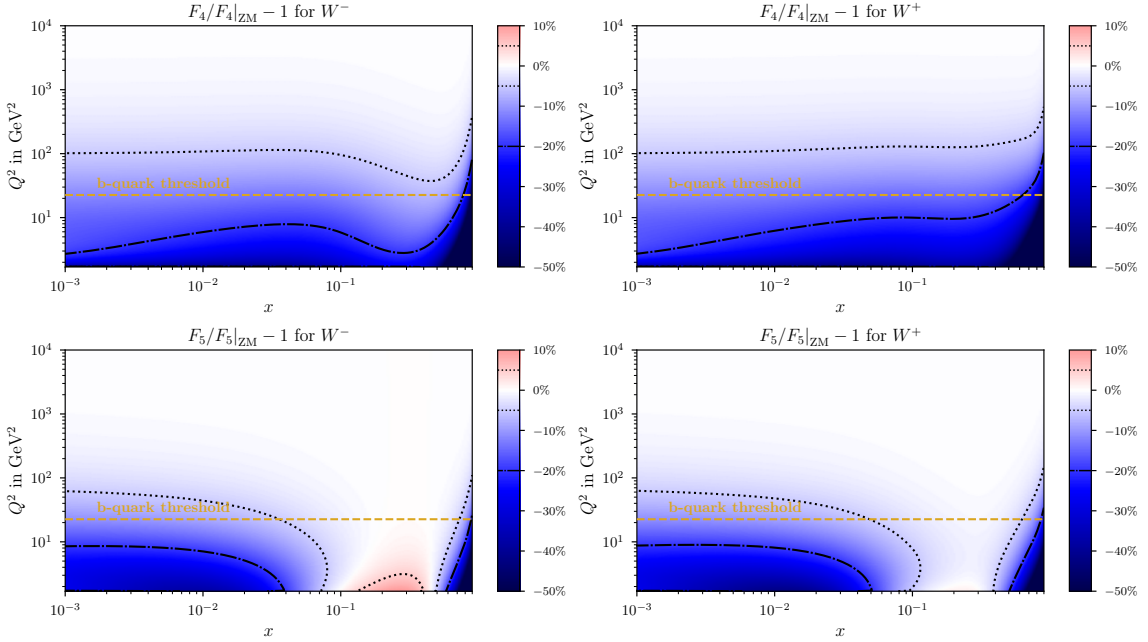


Figure 6: The ratios of eq. (6.9) at NLO for F_4 in the top row and F_5 in the bottom row. The dash-dotted line indicates the -20% difference and the dotted line the -5% difference. Note that all four ratios reach -100% in the bottom right corner.

functions. In fig. 6 we display the ratios

$$\frac{F_4^{W^-}(x, Q^2)}{F_4^{W^-}(x, Q^2)|_{\text{ZM}}} - 1 \quad \text{and} \quad \frac{F_4^{W^+}(x, Q^2)}{F_4^{W^+}(x, Q^2)|_{\text{ZM}}} - 1 \quad (6.9)$$

$$\frac{F_5^{W^-}(x, Q^2)}{F_5^{W^-}(x, Q^2)|_{\text{ZM}}} - 1 \quad \text{and} \quad \frac{F_5^{W^+}(x, Q^2)}{F_5^{W^+}(x, Q^2)|_{\text{ZM}}} - 1 \quad (6.10)$$

as heatmaps. These figures are arranged in the same order as the ratios above. We consider the ratio on a double-logarithmic grid of (400×400) points corresponding to the ranges $Q^2 \in [m_c^2, 10^4]$ GeV^2 and $x \in [10^{-4}, 0.9]$. The lower limit of the Q^2 range is given by the initial scale of the CT18NLO PDFs. Deviations from zero are given in blue for negative values and red for positive values. The dashed-dotted contour indicates -20% difference and the dotted $\pm 5\%$. Note that the color coding for the heatmap is kept the same for all four panels.

The first row, showing F_4 , yields almost uniform suppression across all values of x of the massive calculation compared to the ZM. The mass effects can be very significant at low Q^2 , especially in the bottom-right (high- x) corner, where the ratios almost reach -100%, but diminish quickly. The -5% contour is already found at $Q^2 \approx 10^2 \text{ GeV}^2$ and the -1% contours (not shown in the figure) are at $Q^2 \approx 10^3 \text{ GeV}^2$. The only variation is in the valence region for W^- , where the contour dips towards lower Q^2 values. Since F_4 is, for the most part, given by the GF contribution, a large part of the suppression is easily identified as the mass-reduced phase space given in the equations through the lower integration bound χ' . The second row, showing F_5 , yields a different behavior along the x axes. For low- and very high- x we find a similar suppression as for F_4 , but in the valence region the suppression fades, or, in the case for W^- , even becomes an +5% enhancement. Overall the mass effect die out faster as for F_4 , with the -5% contour reaching up to 80 GeV^2 and the -1% contour (not shown) reaching up to 500 GeV^2 .

7 Conclusions

In this work, we have presented a comprehensive analysis of the deep-inelastic structure functions F_4 and F_5 at NLO in QCD. Our framework incorporated full heavy quark mass effects within the ACOT scheme. We provided both analytic expressions and a detailed numerical implementation, accounting for quark scattering and boson-gluon fusion contributions with full real and virtual corrections.

Our analysis revealed that NLO corrections lead to substantial modifications of leading-order predictions for F_5 , with deviations reaching 25–45% in relevant kinematic regions. In contrast, F_4 is almost entirely generated at NLO, as its leading order contribution is strongly suppressed in the massless limit. These effects are particularly pronounced at low Q^2 and moderate x , where heavy quark mass effects are significant. Specifically, we confirm that F_4 remains suppressed by the quark mass, whereas F_5 exhibits nontrivial behavior, particularly in the presence of heavy flavors. In the large Q^2 region (above $Q^2 = 10^3 \text{ GeV}^2$ for less than 1% correction) we confirm the onset of the AJ relation, which yields a connection between $F_{4/5}$ and the better known $F_{L/2}$.

The theoretical framework and numerical results presented here are directly relevant for upcoming experimental programs, such as the SHiP experiment at CERN and neutrino telescopes like IceCube. These facilities are uniquely sensitive to contributions from F_4 and F_5 via τ -lepton and ν_τ interactions. Consequently, this work establishes a baseline for interpreting future measurements and probing the heavy quark content of the nucleon with unprecedented precision.

Future investigations should address the interplay between NLO corrections, target mass effects, and nuclear corrections to achieve a fully consistent description of DIS structure functions across the entire kinematic range. Furthermore, a quantitative assessment of theoretical uncertainties and an extension to next-to-next-to-leading order will be crucial for maximizing the impact of future experimental data.

Acknowledgments

This work has been supported by the BMBF under contract 05P24PMA. M.K. thanks the School of Physics at the University of New South Wales in Sydney, Australia for its hospitality and financial support through the Gordon Godfrey visitors program. The work of P.R. was supported by the U.S. Department of Energy under Grant No. DE-SC0010129 and by the Office of Science, the Office of Nuclear Physics, within the framework of the Saturated Glue (SURGE) Topical Theory Collaboration. P.R. further thanks the Jefferson Lab for their hospitality. This material is based upon work supported by the U.S. Department of Energy, Office of Science, Office of Nuclear Physics under contract DE-AC05-06OR23177.

A Collinear frame

When investigating the scattering of a space-like vector boson off a nucleon, it is convenient to adopt reference frames where the relevant four-vectors, P and q , lie in the t - z plane. These frames, often referred to as collinear frames, simplify the analysis by aligning the motion along the longitudinal axis. In such frames, it is particularly useful to express the four-vectors using their light-cone coordinate components [40]. In the collinear frame, a general four-vector v^μ can then be written as

$$v^\mu = (v^+, v^-, \mathbf{v}_\perp), \quad (\text{A.1})$$

where the "plus" and "minus" components are defined as

$$v^\pm = \frac{1}{\sqrt{2}}(v^0 \pm v^3) \quad (\text{A.2})$$

and the transverse components are given by $\mathbf{v}_\perp = (v^1, v^2)$. In this coordinate system, the invariant line element becomes

$$ds^2 = 2dx^+dx^- - \delta_{ij}dx^i dx^j \quad \text{with } i, j = 1, 2. \quad (\text{A.3})$$

This metric reflects the separation of longitudinal and transverse components, which is a key feature of light-cone coordinates.

In light-cone coordinates, the four-momenta P^μ and q^μ can be expressed as [41]

$$P^\mu = \left(P^+, \frac{M^2}{2P^+}, \mathbf{0} \right), \quad (\text{A.4})$$

$$q^\mu = \left(-\kappa P^+, \frac{Q^2}{2\kappa P^+}, \mathbf{0} \right), \quad (\text{A.5})$$

where $P^2 = M^2$, and κ is the Nachtmann variable [42] defined through the following relation

$$2P \cdot q = \frac{Q^2}{\kappa} - \kappa M^2. \quad (\text{A.6})$$

In the approximation where nucleon mass corrections are neglected, κ reduces to the Bjorken- x variable. Using $k_1^+ = \xi P^+$, we can express the four-vector k_1^μ as

$$k_1^\mu = \left(\xi P^+, \frac{m_1^2}{2\xi P^+}, \mathbf{0} \right). \quad (\text{A.7})$$

With this, and utilizing the relations for P and q in eqs. (A.4) and (A.5), together with the metric defined earlier in eq. (A.3), we obtain the scalar products that are necessary for deriving the results in eqs. (3.32) and (3.33)

$$\begin{aligned} k_1 \cdot q &= \frac{\xi Q^2}{2x} - \frac{m_1^2 x}{2\xi}, \\ q \cdot P &= \frac{Q^2}{2x}, \\ k_1 \cdot P &= \frac{m_1^2}{2\xi}. \end{aligned} \quad (\text{A.8})$$

Keeping the parton mass m_1 explicit is crucial, as it underlies the mixing of partonic structure functions and gives rise to the corresponding terms in eqs. (3.32) and (3.33).

B $\hat{\mathcal{F}}_2^{\text{QS, NLO}}$

The partonic structure function \hat{F}_2^{QS} appears in the mixing terms within the expressions provided in eqs. (3.32) and (3.33). The analytical expression for this function is given by [9]:

$$\begin{aligned} \hat{F}_2^{\text{QS}}(\hat{s}_1, \hat{t}_1) = & 8 \frac{Q^2}{\hat{x} \Delta'^4} \left\{ -2 \Delta^4 q_+ \left(\frac{m_2^2}{\hat{s}_1^2} + \frac{m_1^2}{\hat{t}_1^2} + \frac{\Sigma_{++}}{\hat{s}_1 \hat{t}_1} \right) + 2 m_1 m_2 q_- \left(\frac{(\Delta'^2 - 6 m_1^2 Q^2) \hat{s}_1}{\hat{t}_1} \right. \right. \\ & + 2 (\Delta'^2 - 3 Q^2 (\hat{s}_1 + \Sigma_{++})) + \hat{t}_1 \frac{\Delta'^2 - 6 Q^2 (m_2^2 + \hat{s}_1)}{\hat{s}_1} \left. \right) \\ & + q_+ \left(\frac{-2 m_1^2 \hat{s}_1 [(\Delta^2 - 6 m_1^2 Q^2) \hat{s}_1 + 2 \Delta^2 \Sigma_{+-}]}{\hat{t}_1^2} + \frac{-2 \Delta^2 (\Delta^2 + 2 \Sigma_{+-} \Sigma_{++})}{\hat{t}_1} \right. \\ & + \frac{-\hat{s}_1 [2 (\Delta^2 - 6 m_1^2 Q^2) \hat{s}_1 + (\Delta'^2 - 18 m_1^2 Q^2) \Sigma_{++} + 2 \Delta^2 (3 \Sigma_{++} - 4 m_1^2)]}{\hat{t}_1} \\ & \left. \left. + \left[-2 (m_1^2 + m_2^2) \hat{s}_1^2 - 9 m_2^2 \Sigma_{+-}^2 - \frac{2 \Delta^2 (\Delta^2 + 2 m_2^2 \Sigma_{+-})}{\hat{s}_1} + 2 \hat{s}_1 [2 \Delta^2 \right. \right. \right. \\ & \left. \left. \left. + (m_1^2 - 5 m_2^2) \Sigma_{+-}] + \Delta^2 (2 \Sigma_{++} - m_2^2) \right] - \hat{t}_1 \frac{[\Delta'^2 - 6 Q^2 (m_2^2 + \hat{s}_1)] \Sigma_{++}}{\hat{s}_1} \right) \right\}, \end{aligned} \quad (\text{B.1})$$

from which we obtain

$$\hat{F}_2^{\text{QS, NLO}}(\xi') = C_F \left(N_2 (S_2 + V_2) \delta(1 - \xi') + \frac{1}{8} \frac{1 - \xi'}{(1 - \xi')_+} \frac{\hat{s}_1}{\hat{s}_1 + m_2^2} \hat{F}_2^{\text{QS}}(\hat{s}_1) \right). \quad (\text{B.2})$$

The coefficients are given by

$$V_2 = \left(C_{R,-} + \frac{1}{2} (m_2^2 C_{1,-} + m_1^2 C_{1,+}) \right) + \frac{q_-}{q_+} \left(\frac{1}{2} m_1 m_2 (C_{1,-} + C_{1,+}) + C_+ \right), \quad S_2 = S_5, \quad N_2 = N_5. \quad (\text{B.3})$$

C Plus-distribution identities

This appendix collects useful properties of plus distributions, which are essential for manipulating convolution kernels in the main text. We use the following definition [43]:

$$[p(x)]_+ = \lim_{\epsilon \rightarrow 0} \left(\theta(1 - \epsilon - x) p(x) - \delta(1 - \epsilon - x) \int_0^{1-\epsilon} dy p(y) \right). \quad (\text{C.1})$$

and the plus distribution over $[\chi, 1]$ with weight s is defined as:

$$([p]_+ s \otimes f)(\chi) := \int_\chi^1 dz [p(z)]_+ s(z) f\left(\frac{\chi}{z}\right). \quad (\text{C.2})$$

From the definition, the following identities hold:

$$(A(x) + B(x))|_+ = A(x)|_+ + B(x)|_+, \quad (\text{C.3})$$

$$(c p(x))|_+ = c p(x)|_+ \quad (c \in \mathbb{R}), \quad (\text{C.4})$$

$$(p(x)|_+)|_+ = p(x)|_+. \quad (\text{C.5})$$

These reflect linearity, homogeneity, and idempotence.

The following lemmas are key for our work:

Lemma 1 (Convolution Identity). *The convolution of a plus distribution with weight $s(z)$ over $[\chi, 1]$ satisfies:*

$$([p]_+ s \otimes f)(\chi) = \int_{\chi}^1 dz p(z) \left[s(z) f\left(\frac{\chi}{z}\right) - s(1) f(\chi) \right] - s(1) f(\chi) \int_0^{\chi} dz p(z). \quad (\text{C.6})$$

Proof.

$$\begin{aligned} & [([p]_+ s) \otimes f](\chi) \stackrel{\text{def}}{=} \int_{\chi}^1 dz [p(z)]_+ s(z) f\left(\frac{\chi}{z}\right) \\ &= \int_{\chi}^1 dz \lim_{\epsilon \rightarrow 0} \left(\theta(1 - \epsilon - z) p(z) - \delta(1 - \epsilon - z) \int_0^{1-\epsilon} dx p(x) \right) s(z) f\left(\frac{\chi}{z}\right) \\ &= \lim_{\epsilon \rightarrow 0} \int_{\tilde{\chi}}^{1-\epsilon} dz p(z) s(z) f\left(\frac{\chi}{z}\right) - \int_{\chi}^1 dz \lim_{\epsilon \rightarrow 0} \delta(1 - \epsilon - z) \int_0^{1-\epsilon} dx p(x) s(z) f\left(\frac{\chi}{z}\right) \\ &= \int_{\chi}^1 dz p(z) \left(s(z) f\left(\frac{\chi}{z}\right) - s(1) f(\chi) \right) + s(1) f(\chi) \lim_{\epsilon \rightarrow 0} \int_{\chi}^{1-\epsilon} dz p(z) \\ &\quad - \lim_{\epsilon \rightarrow 0} \int_0^{1-\epsilon} dx p(x) \int_{\tilde{\chi}}^1 dz \delta(1 - \epsilon - z) s(z) f\left(\frac{\chi}{z}\right) \\ &= \int_{\chi}^1 dz p(z) \left(s(z) f\left(\frac{\chi}{z}\right) - s(1) f(\chi) \right) + s(1) f(\chi) \lim_{\epsilon \rightarrow 0} \int_{\chi}^{1-\epsilon} dz p(z) \\ &\quad - \lim_{\epsilon \rightarrow 0} \int_0^{1-\epsilon} dx p(x) s(1 - \epsilon) f\left(\frac{\chi}{1 - \epsilon}\right) \\ &= \int_{\chi}^1 dz p(z) \left(s(z) f\left(\frac{\chi}{z}\right) - s(1) f(\chi) \right) + s(1) f(\chi) \lim_{\epsilon \rightarrow 0} \int_{\chi}^{1-\epsilon} dz p(z) \\ &\quad - \left(s(1) f(\chi) \lim_{\epsilon \rightarrow 0} \int_{\chi}^{1-\epsilon} dz p(z) + s(1) f(\chi) \int_0^{\chi} dz p(z) \right) \\ &= \int_{\chi}^1 dz p(z) \left(s(z) f\left(\frac{\chi}{z}\right) - s(1) f(\chi) \right) - s(1) f(\chi) \int_0^{\chi} dz p(z). \end{aligned} \quad (\text{C.7})$$

□

Lemma 2 (Product Rule). *Let $s_1(x)$ be smooth at $x = 1$, and let $p_1(x)$ be a kernel with plus prescription. Then, as distributions:*

$$(p_1(x) s_1(x))|_+ = s_1(x) p_1(x)|_+ + \delta(1 - x) \int_0^1 dy p_1(y) [s_1(1) - s_1(y)]. \quad (\text{C.8})$$

Proof. Define $P(x) := p_1(x) s_1(x)$. The convolution is

$$(P \otimes f)(x) = \int_x^1 dy p_1(y) s_1(y) [f(x/y) - f(x)] - f(x) \int_0^x dy p_1(y) s_1(y).$$

The weighted plus convolution is

$$(p_1|_+ s_1) \otimes f(x) = \int_x^1 dy p_1(y) [s_1(y) f(x/y) - s_1(1) f(x)] - f(x) s_1(1) \int_0^x dy p_1(y).$$

Subtracting gives

$$\begin{aligned}
& (P \otimes f)(x) - (p_1|_+ s_1) \otimes f(x) \\
&= f(x) \left[\int_x^1 dy p_1(y) (s_1(1) - s_1(y)) + \int_0^x dy p_1(y) (s_1(1) - s_1(y)) \right] \\
&= f(x) \int_0^1 dy p_1(y) (s_1(1) - s_1(y)),
\end{aligned}$$

which is a $\delta(1 - x)$ term with the coefficient in eq. (C.8). \square

D Numerical implementation of the plus distribution

This appendix details the numerical treatment of the convolution integrals appearing in the NLO QS processes. The accurate evaluation of these integrals requires a careful handling of the plus distribution arising in the hard scattering Wilson coefficients.

The convolution integrals for the structure functions are expressed as

$$F_{i,\alpha,\beta}^{\text{QS, NLO, } k}(x, Q^2) = \frac{\alpha_s}{2\pi} \int_\chi^1 d\xi' f_\alpha \left(\frac{\chi}{\xi'}, Q^2 \right) \mathcal{H}_{i,\alpha,\beta}^{\text{QS, NLO, } k}(\xi'), \quad (\text{D.1})$$

$$\mathcal{H}_{i,\alpha,\beta}^{\text{QS, NLO, } k}(\xi') = L_{i,\alpha,\beta}^k \delta(1 - \xi') + [p_1(\xi')]_+ S_{1,i,\alpha,\beta}^k(\xi'), \quad (\text{D.2})$$

where $p_1(\xi') = 1/(1 - \xi')$ and

$$S_{1,4,\alpha,\beta}^k(\xi') = \mathcal{K} \left(\hat{F}_{4,\alpha,\beta}^{\text{QS, } k}(\xi') + (\mathcal{R}_2 - 1) \left(\mathcal{R}_1 \hat{F}_{2,\alpha,\beta}^{\text{QS, } k}(\xi') + \hat{F}_{5,\alpha,\beta}^{\text{QS, } k}(\xi') \right) \right) \quad (\text{D.3})$$

$$S_{1,5,\alpha,\beta}^k(\xi') = \mathcal{K} \mathcal{R}_2 \left(\hat{F}_{5,\alpha,\beta}^{\text{QS, } k}(\xi') + 2\mathcal{R}_1 \hat{F}_{2,\alpha,\beta}^{\text{QS, } k}(\xi') \right) \quad (\text{D.4})$$

with

$$\mathcal{K} = \frac{1}{8} (1 - \xi') \frac{\hat{s}_1}{\hat{s}_1 + m_2^2}. \quad (\text{D.5})$$

The coefficients $L_{i,\alpha,\beta}^k$ are given by

$$L_{2,\alpha,\beta}^k = \chi \frac{(1 + \bar{\mathcal{R}}_3)^2}{(1 - \bar{\mathcal{R}}_3)} \hat{N}_{2,\alpha,\beta}^k, \quad (\text{D.6})$$

$$L_{4,\alpha,\beta}^k = \hat{N}_{4,\alpha,\beta}^k + (\bar{\mathcal{R}}_2 - 1) (\bar{\mathcal{R}}_1 \hat{N}_{2,\alpha,\beta}^k + \hat{N}_{5,\alpha,\beta}^k), \quad (\text{D.7})$$

$$L_{5,\alpha,\beta}^k = \bar{\mathcal{R}}_2 (\hat{N}_{5,\alpha,\beta}^k + 2\bar{\mathcal{R}}_1 \hat{N}_{2,\alpha,\beta}^k), \quad (\text{D.8})$$

where $\bar{\mathcal{R}}_i$ are the R_i coefficients evaluated at $\xi' = 1$, and

$$\hat{N}_{2,\alpha,\beta}^k = N_{2,\alpha,\beta}^k (V_{2,\alpha,\beta} + S_{2,\alpha,\beta}), \quad (\text{D.9})$$

$$\hat{N}_{4,\alpha,\beta}^k = N_{4,\alpha,\beta}^k V_{4,\alpha,\beta}, \quad (\text{D.10})$$

$$\hat{N}_{5,\alpha,\beta}^k = N_{5,\alpha,\beta}^k (V_{5,\alpha,\beta} + S_{5,\alpha,\beta}). \quad (\text{D.11})$$

Note that $S_4 = 0$ and that we use the index convention of eq. (6.1).

Using the identities for the plus distribution, the convolution products can be expressed as follows, which also directly corresponds to their implementation in the code:

$$F_{i,\alpha,\beta}^{\text{QS, NLO, } k}(x, Q^2) = \frac{\alpha_s}{2\pi} \left[\mathcal{L}_{1,i,\alpha,\beta}^k f_\alpha(\chi) + \int_\chi^1 \frac{S_{1,i,\alpha,\beta}^k(\xi')}{1 - \xi'} \left(f_\alpha \left(\frac{\chi}{\xi'} \right) - f_\alpha(\chi) \right) d\xi' \right], \quad (\text{D.12})$$

with

$$\mathcal{L}_{1,i,\alpha,\beta}^k = L_{i,\alpha,\beta}^k + \ln(1-\chi) \bar{S}_{1,i,\alpha,\beta}^k + \int_{\chi}^1 \frac{S_{1,i,\alpha,\beta}^k(\xi') - \bar{S}_{1,i,\alpha,\beta}^k}{1-\xi'} d\xi'. \quad (\text{D.13})$$

The coefficients $\bar{S}_{1,\alpha,\beta}^k$ are given by

$$\bar{S}_{1,1,\alpha,\beta}^k = \chi \frac{(1+\bar{\mathcal{R}}_3)^2}{(1-\bar{\mathcal{R}}_3)} \hat{S}_{1,1,\alpha,\beta}^k, \quad (\text{D.14})$$

$$\bar{S}_{1,4,\alpha,\beta}^k = \hat{S}_{1,4,\alpha,\beta}^k + (\bar{R}_2 - 1)(\bar{R}_1 \hat{S}_{1,2,\alpha,\beta}^k + \hat{S}_{1,5,\alpha,\beta}^k), \quad (\text{D.15})$$

$$\bar{S}_{1,5,\alpha,\beta}^k = \bar{\mathcal{R}}_2 (\hat{S}_{1,5,\alpha,\beta}^k + 2\bar{\mathcal{R}}_1 \hat{S}_{1,2,\alpha,\beta}^k). \quad (\text{D.16})$$

where

$$\hat{S}_{1,2,\alpha,\beta}^k = -2N_{2,\alpha,\beta}^k (2 - \Sigma_{++} I_1), \quad (\text{D.17})$$

$$\hat{S}_{1,4,\alpha,\beta}^k = 0, \quad (\text{D.18})$$

$$\hat{S}_{1,5,\alpha,\beta}^k = -2N_{5,\alpha,\beta}^k (2 - \Sigma_{++} I_1), \quad (\text{D.19})$$

Note that the coefficients $\hat{S}_{1,i}$ can also be derived from

$$\hat{S}_{1,i,\alpha,\beta}^k = \lim_{\hat{s}_1 \rightarrow 0} \left[-2N_{i,\alpha,\beta}^k \frac{\hat{s}_1^2}{m_2^2} \int_0^1 \left(\frac{m_2^2}{\hat{s}_1^2} + \frac{m_1^2}{\hat{t}_1^2} + \frac{\Sigma_{++}}{\hat{s}_1 \hat{t}_1} \right) dy \right] \quad (\text{D.20})$$

$$= -2N_{i,\alpha,\beta}^k (2 - \Sigma_{++} I_1). \quad (\text{D.21})$$

Following the same logic for the subtraction term:

$$F_{i,\alpha,\beta}^{\text{QS, SUB}, k}(x, Q^2) = \mathcal{N}_{i,\alpha,\beta}^{\text{QS, LO}, k} \times \frac{\alpha_s}{2\pi} \int_{\chi}^1 d\xi' f_{\alpha} \left(\frac{\chi}{\xi'}, \mu^2 \right) \mathcal{H}_{i,\alpha}^{\text{QS, SUB}, k}(\xi'), \quad (\text{D.22})$$

$$\mathcal{H}_{i,\alpha}^{\text{QS, SUB}, k}(\xi') = c_i C_F \left[\frac{1+\xi'^2}{1-\xi'} \left(\ln \frac{Q^2}{m_{\alpha}^2} - 1 - 2 \ln(1-\xi') \right) \right]_{+}. \quad (\text{D.23})$$

with $c_4 = 0$, $c_5 = 1$ we can write:

$$F_{i,\alpha,\beta}^{\text{QS, SUB}, k}(x, Q^2) = \mathcal{N}_{i,\alpha,\beta}^{\text{QS, LO}, k} \times \frac{\alpha_s}{2\pi} \left[P_{2,i,\alpha}(\chi) f(\chi) + \int_{\chi}^1 p_{2,i,\alpha}(\xi') \left(f_{\alpha} \left(\frac{\chi}{\xi'} \right) - f_{\alpha}(\chi) \right) d\xi' \right], \quad (\text{D.24})$$

where

$$p_{2,i,\alpha}(\xi') = c_i C_F \frac{1+\xi'^2}{1-\xi'} \left(\ln \frac{Q^2}{m_{\alpha}^2} - 1 - 2 \ln(1-\xi') \right), \quad (\text{D.25})$$

$$\begin{aligned} P_{2,i,\alpha}(\chi) &= - \int_0^{\chi} p_{2,i,\alpha}(\xi') d\xi' \\ &= c_i C_F \left[2\chi + \ln \left(\frac{Q^2}{m_{\alpha}^2} \right) \left(\frac{\chi(2+\chi)}{2} + 2 \ln(1-\chi) \right) - \ln(1-\chi) (-1 + \chi(2+\chi) + 2 \ln(1-\chi)) \right] \end{aligned} \quad (\text{D.26})$$

Note the emergence of the logarithmic terms $\ln(1-\chi)$ and $\ln^2(1-\chi)$ in eqs. (D.13) and (D.26) corresponds to the soft-gluon instabilities previously outlined in the main text, *cf. sec. 6*.

References

- [1] **Particle Data Group** Collaboration, S. Navas et al., *Review of particle physics*, *Phys. Rev. D* **110** (2024), no. 3 030001.
- [2] S. Collaboration, *The ship experiment at the proposed cern sps beam dump facility*, 2022.
- [3] **IceCube** Collaboration, R. Abbasi et al., *Observation of Seven Astrophysical Tau Neutrino Candidates with IceCube*, *Phys. Rev. Lett.* **132** (2024), no. 15 151001, [[arXiv:2403.02516](https://arxiv.org/abs/2403.02516)].
- [4] R. Mammen Abraham et al., *Tau neutrinos in the next decade: from GeV to EeV*, *J. Phys. G* **49** (2022), no. 11 110501, [[arXiv:2203.05591](https://arxiv.org/abs/2203.05591)].
- [5] M. A. G. Aivazis, F. I. Olness, and W.-K. Tung, *Leptoproduction of heavy quarks. 1. General formalism and kinematics of charged current and neutral current production processes*, *Phys. Rev. D* **50** (1994) 3085–3101, [[hep-ph/9312318](https://arxiv.org/abs/hep-ph/9312318)].
- [6] M. A. G. Aivazis, J. C. Collins, F. I. Olness, and W.-K. Tung, *Leptoproduction of heavy quarks. 2. A Unified QCD formulation of charged and neutral current processes from fixed target to collider energies*, *Phys. Rev. D* **50** (1994) 3102–3118, [[hep-ph/9312319](https://arxiv.org/abs/hep-ph/9312319)].
- [7] J. C. Collins, *Hard scattering factorization with heavy quarks: A General treatment*, *Phys. Rev. D* **58** (1998) 094002, [[hep-ph/9806259](https://arxiv.org/abs/hep-ph/9806259)].
- [8] Y. S. Jeong and M. H. Reno, *Neutrino cross sections: Interface of shallow- and deep-inelastic scattering for collider neutrinos*, 2023.
- [9] S. Kretzer and I. Schienbein, *Heavy quark initiated contributions to deep inelastic structure functions*, *Phys. Rev. D* **58** (1998) 094035, [[hep-ph/9805233](https://arxiv.org/abs/hep-ph/9805233)].
- [10] R. Mertig, M. Böhm, and A. Denner, *Feyn calc - computer-algebraic calculation of feynman amplitudes*, *Computer Physics Communications* **64** (1991), no. 3 345–359.
- [11] V. Shtabovenko, R. Mertig, and F. Orellana, *New developments in feyncalc 9.0*, *Computer Physics Communications* **207** (Oct., 2016) 432–444.
- [12] V. Shtabovenko, R. Mertig, and F. Orellana, *Feyncalc 9.3: New features and improvements*, *Computer Physics Communications* **256** (Nov., 2020) 107478.
- [13] V. Shtabovenko, R. Mertig, and F. Orellana, *Feyncalc 10: Do multiloop integrals dream of computer codes?*, *Computer Physics Communications* **306** (Jan., 2025) 109357.
- [14] J. C. Collins, *Renormalization : An Introduction to Renormalization, the Renormalization Group and the Operator-Product Expansion*, vol. 26 of *Cambridge Monographs on Mathematical Physics*. Cambridge University Press, Cambridge, 1984.
- [15] W. Furmanski and R. Petronzio, *Lepton - Hadron Processes Beyond Leading Order in Quantum Chromodynamics*, *Z. Phys. C* **11** (1982) 293.
- [16] M. E. Peskin and D. V. Schroeder, *An Introduction to quantum field theory*. Addison-Wesley, Reading, USA, 1995.
- [17] T. Kinoshita, *Mass singularities of Feynman amplitudes*, *J. Math. Phys.* **3** (1962) 650–677.
- [18] T. D. Lee and M. Nauenberg, *Degenerate Systems and Mass Singularities*, *Physical Review* **133** (Mar., 1964) B1549–B1562.
- [19] S. Kretzer and I. Schienbein, *Heavy quark fragmentation in deep inelastic scattering*, *Phys. Rev. D* **59** (1999) 054004, [[hep-ph/9808375](https://arxiv.org/abs/hep-ph/9808375)].
- [20] G. Passarino and M. Veltman, *One-loop corrections for e+e- annihilation into $\mu^+\mu^-$ in the weinberg model*, *Nuclear Physics B* **160** (1979), no. 1 151–207.
- [21] T. Gottschalk, *Chromodynamic corrections to neutrino production of heavy quarks*, *Phys. Rev. D* **23** (Jan, 1981) 56–74.

- [22] G. Altarelli, R. K. Ellis, and G. Martinelli, *Large Perturbative Corrections to the Drell-Yan Process in QCD*, *Nucl. Phys. B* **157** (1979) 461–497.
- [23] W. A. Bardeen, A. J. Buras, D. W. Duke, and T. Muta, *Deep Inelastic Scattering Beyond the Leading Order in Asymptotically Free Gauge Theories*, *Phys. Rev. D* **18** (1978) 3998.
- [24] J. C. Collins, D. E. Soper, and G. Sterman, *Factorization of hard processes in qcd*, 2004.
- [25] J. D. Bjorken, *Asymptotic sum rules at infinite momentum*, *Phys. Rev.* **179** (Mar, 1969) 1547–1553.
- [26] C. Albright and C. Jarlskog, *Neutrino production of $m+$ and $e+$ heavy leptons (i)*, *Nuclear Physics B* **84** (1975), no. 2 467–492.
- [27] G. Altarelli and G. Parisi, *Asymptotic Freedom in Parton Language*, *Nucl. Phys. B* **126** (1977) 298–318.
- [28] J. C. Collins, D. E. Soper, and G. F. Sterman, *Factorization of Hard Processes in QCD*, *Adv. Ser. Direct. High Energy Phys.* **5** (1989) 1–91, [[hep-ph/0409313](#)].
- [29] B. Mele and P. Nason, *The fragmentation function for heavy quarks in QCD*, *Nuclear Physics B* **361** (Jan., 1991) 626–644.
- [30] J. Collins, F. Wilczek, and A. Zee, *Low-energy manifestations of heavy particles: Application to the neutral current*, *Phys. Rev. D* **18** (Jul, 1978) 242–247.
- [31] S. Kretzer and M. H. Reno, *Tau neutrino deep inelastic charged current interactions*, *Physical Review D* **66** (Dec., 2002).
- [32] **APFEL** Collaboration, V. Bertone, S. Carrazza, and J. Rojo, *APFEL: A PDF Evolution Library with QED corrections*, *Comput. Phys. Commun.* **185** (2014) 1647–1668, [[arXiv:1310.1394](#)].
- [33] V. Bertone, *APFEL++: A new PDF evolution library in C++*, *PoS DIS2017* (2018) 201, [[arXiv:1708.00911](#)].
- [34] V. Bertone, “apfelxx.” <https://github.com/vbertone/apfelxx>, 2017.
- [35] F. Halzen and A. D. Martin, *Quarks and Leptons: An Introductory Course in Modern Particle Physics*. John Wiley & Sons, New York, 1984.
- [36] T.-J. Hou et al., *New CTEQ global analysis of quantum chromodynamics with high-precision data from the LHC*, *Phys. Rev. D* **103** (2021), no. 1 014013, [[arXiv:1912.10053](#)].
- [37] A. Buckley, J. Ferrando, S. Lloyd, K. Nordström, B. Page, M. Rüfenacht, M. Schönherr, and G. Watt, *LHAPDF6: parton density access in the LHC precision era*, *Eur. Phys. J. C* **75** (2015) 132, [[arXiv:1412.7420](#)].
- [38] S. Catani and L. Trentadue, *Resummation of the QCD Perturbative Series for Hard Processes*, *Nucl. Phys. B* **327** (1989) 323–352.
- [39] S. Moch and A. Vogt, *Threshold resummation of the structure function*, *Journal of High Energy Physics* **2009** (Apr., 2009) 081–081.
- [40] P. A. M. Dirac, *Forms of relativistic dynamics*, *Rev. Mod. Phys.* **21** (Jul, 1949) 392–399.
- [41] R. Ellis, W. Furmanski, and R. Petronzio, *Unravelling higher twists*, *Nuclear Physics B* **212** (1983), no. 1 29–98.
- [42] O. Nachtmann, *Positivity constraints for anomalous dimensions*, *Nucl. Phys. B* **63** (1973) 237–247.
- [43] R. D. Field, *Applications of Perturbative QCD*, vol. 77. 1989.